Organic/Organometallic Hybrids as Broadband Nonlinear Transmission Materials.

Final Report

Grant #: W911NF-06-2-0032
7/1/06 – 6/30/10

PI: Dr. Wenfang Sun
North Dakota State University

A. Technical Report

The ultimate goal of this project is to understand the structure-property correlation in organometallic complexes in order to develop broadband nonlinear transmission materials. To realize this goal, we have synthesized and performed systematic photophysical study and nonlinear optical characterization of 87 square-planar platinum terdentate/bidentate complexes, 5 texaphyrin derivatives, and 6 stilbazolium derivatives. In addition, we investigated the photophysics and nonlinear absorption of 10 other platinum complexes and 10 zinc phthalocyanine derivatives provided by collaborators in China. From these studies, we have discovered that in order to improve the reverse saturable absorption, reducing the ground-state absorption is critical. To expand the nonlinear absorption spectral region from the visible to the near-IR for the platinum complexes, we incorporated substituted fluorene component to the terdentate ligand or acetylide ligand(s) in order to utilize the reverse saturable absorption in the visible and two-photon induced excited-state absorption in the near-IR region. Several platinum complexes synthesized by our group exhibit the largest ratio of excited-state absorption to ground-state absorption cross section and the largest two-photon absorption cross-sections ever reported for organometallic complexes. They are the most promising broadband nonlinear absorption organometallic complexes reported to date. One of them have been used for ARL field test and exhibit promising results.

A.1. Synthesis, photophysics and nonlinear absorption of platinum terdentate/bidentate complexes

Complexes **1-10** were synthesized to investigate how the improved co-planarity and conjugation between the aryl substituent and the terdentate ligand influence the photophysics and nonlinear absorption. It was found that the improved co-planarity and conjugation caused the red-shift of the metal-to-ligand charge transfer (MLCT) band. Therefore, the reverse saturable absorption was reduced due to the decreased ratio of the excited-state absorption to the ground-state absorption cross section (σ_{ex}/σ_0). The details for these studies were described in our publications #17 and 20.

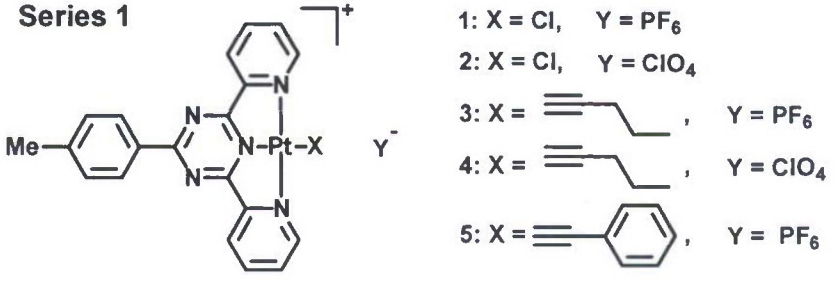

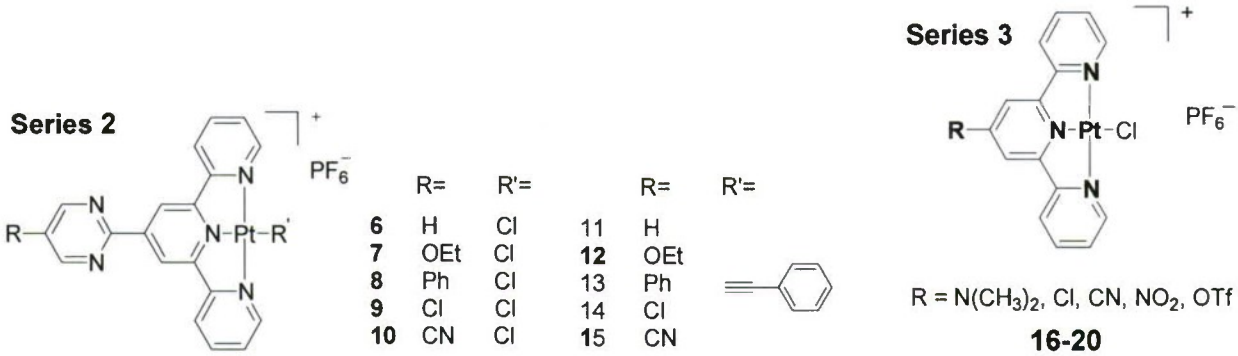

Complexes **16-20** were designed and synthesized to investigate the effect of substituent at the 4-position of the terpyridyl ligand on the excited-state properties. It was discovered that strong electron-donating substituent $N(CH_3)_2$ admixes intraligand charge transfer (ILCT) character and MLCT character. Therefore, the lifetime of the triplet excited state is greatly increased, which in turn enhances the reverse saturable absorption of this complex. The details of the study based on this series of complexes were reported in our publication #12.

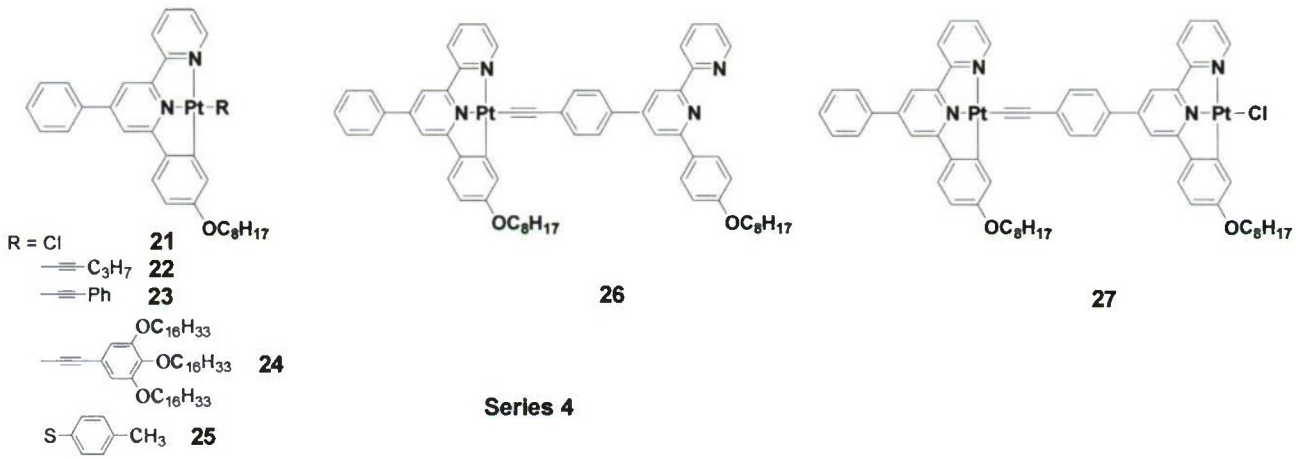

We previously discovered that Pt(II) complexes with C^N^N ligand (6-phenyl-2,2'-bipyridine) exhibit broader excited-state absorption than the corresponding Pt(II) terpyridyl complexes. One of the representative complexes is complex **74** (see publication #16). However, the limited solubility of this complex prevents the population of the excited-state absorption from one-photon absorption. To overcome this disadvantage, we introduced an alkoxyl substituent on the phenyl ring. A variety of monodentate ligands (chloride, acetylide, and thiolate) were investigated to understand the effect of the monodentate ligand on the excited-state properties, especially the nonlinear absorption. Our studies revealed that the alkoxyl substituent did significantly improve the solubility of the complexes in organic solvents. More importantly, due to the electron-donating ability of the alkoxyl substituent, it increased the ILCT percentage in the lowest excited-state. Therefore, the triplet excited-state lifetimes for complexes **21-23** became much longer in comparison to their corresponding C^N^N complexes without the alkoxyl substituent. The increased electron-donating ability of the monodentate ligand caused the red-shift

of the low-energy charge-transfer absorption band, which resulted in reduced σ_{ex}/σ_0 and consequently reduced reverse saturable absorption at 532 nm. In addition, introducing the alkoxyl substituent made the complexes amphiphilic. We demonstrated that complex **21** can be made into LB films, which is important for the future device applications. The details of these studies were reported in publications #9 and #10. The UV-vis absorption spectra, emission spectra, triplet transient difference absorption spectra and the nonlinear transmission plot for **21-23**, **26** and **27** are provided in Figure 1.

Table 1. Photophysical parameters of **21-23, 26 and 27** at room temperature in CH_2Cl_2 and CH_3CN.

	CH_2Cl_2			CH_3CN		
	λ_{abs} / nm (ε / $M^{-1}cm^{-1}$)	λ_{em} / nm (τ_{em}/ns; Φ_{em}; k_r [a] /s^{-1})	k_q [b] / M^{-1} s^{-1}	λ_{em} / nm (τ_{em}/ns; Φ_{em}; k_r [a] /s^{-1})	λ_{T1-Tn} / nm (τ_T/ns; ε_{T1-Tn} [c] / $M^{-1}cm^{-1}$)	Φ_T [d]
21	286 (40800), 300 (43000), 367 (17200), 431 (3840)	590 (740; 0.033; 4.46×10^4)	1.70×10^9	590 (460; 0.006; 1.30×10^4)	400 (310; 10310), 468 (300; 2950), 670	0.27
22	293 (45300), 342 (17600), 368 (18100), 439 (5800), 464 (5040)	596 (670; 0.19; 2.84×10^5)	1.90×10^9	592 (570; 0.035; 6.14×10^4)	400 (500; 8330), 502 (540; 3100) 680, 798	0.34
23	292 (52000), 344 (17800), 366 (19000), 439 (7240), 464 (6570)	590 (980; 0.15; 1.53×10^5)	2.17×10^9	588 (600; 0.032; 5.33×10^4)	405 (660; 8220), 505, 630 (670; 8660), 670	0.42
26	294 (72300), 329 (57100), 441 (11400), 464 (10600)	590 (970; 0.21; 2.16×10^5)	2.01×10^9	588 (660; 0.052; 7.88×10^4)	400 (720; 19730), 495, 650 (750; 2900), 670, 790	0.11
27	286 (59400), 299 (60000), 366 (30100), 436 (11300)	592 (870; 0.008; 9.20×10^3)	2.47×10^9	584 (510; 0.007; 1.37×10^4)	402, 472, 590 (4830; 2650), 656	0.06
76		596 (400; 0.08; 2.00×10^5)		589 (100; 0.025; 2.50×10^5)	385 (86), 585 (87, 4933)[e]	0.51 [e]

[a] Radiative decay rate constant ($k_r = \Phi/\tau$). [b] Emission self-quenching rate constant. [c] The Triplet excited-state absorption coefficient. [d] The triplet excited-state formation quantum yield. [e] From publication #16.

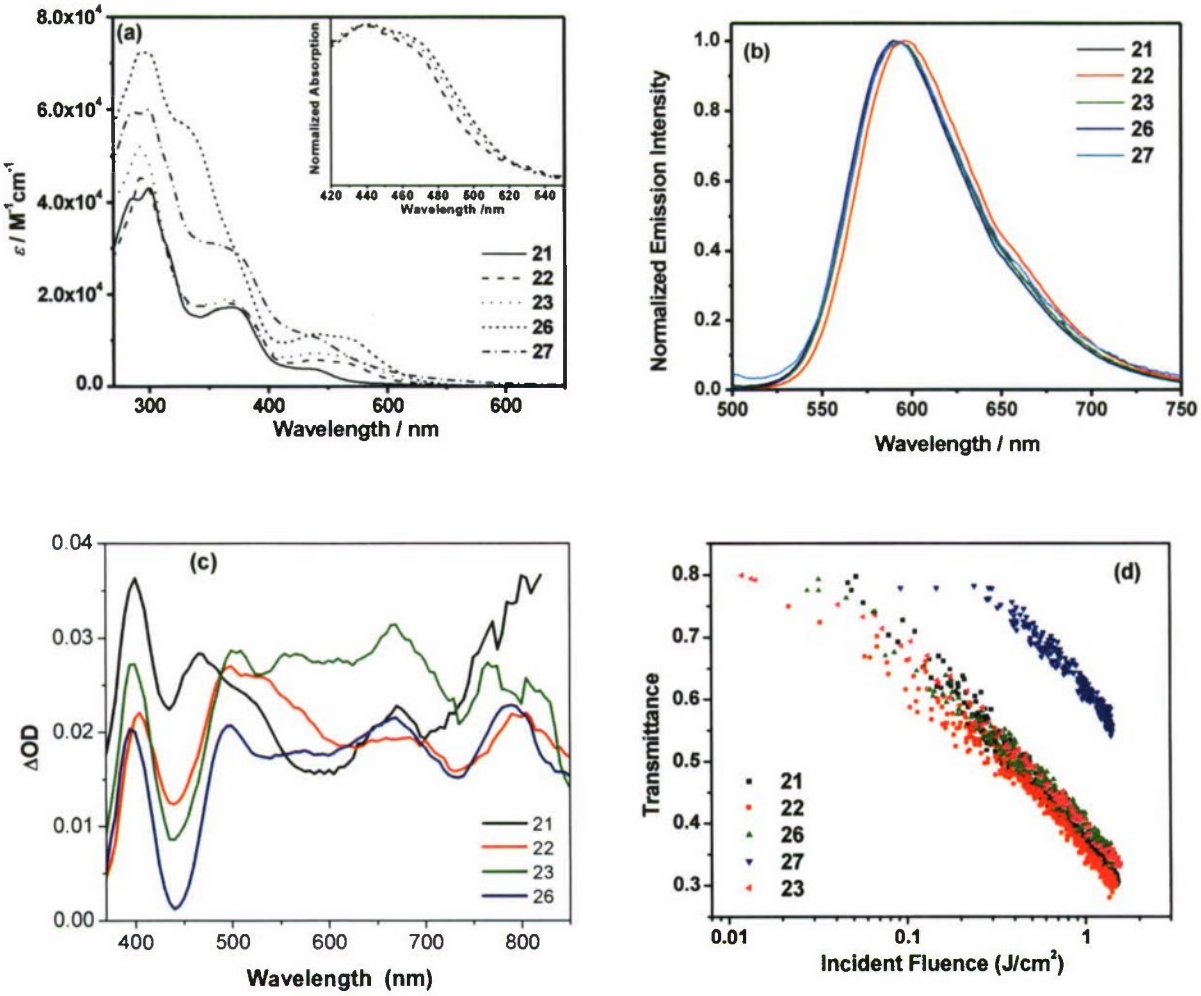

Figure 1. (a) UV-vis absorption spectra in CH_2Cl_2, (b) emission spectra in CH_2Cl_2 at room temperature, (c) ns transient difference absorption spectra in CH_3CN, (d) nonlinear transmission at 532 nm for ns laser pulses in a 2-mm cell in CH_2Cl_2 for **21-23**, **26** and **27**.

Although the solubility of complexes **21-27** was significantly improved, the lack of ground-state absorption in the near-IR region still limited their application as broadband nonlinear absorbing materials. To solve this problem, two approaches were employed. Our first approach was to introduce fluorenyl substituent on the terdentate ligand because the π-donating ability of the fluorenyl substituent could admix intraligand charge transfer character with the ^{1}MLCT state, with could increase the excited-state lifetime. In addition, fluorene-containing molecules with electron-donor and acceptor were found to exhibit moderate to large two-photon absorption. Moreover, the length of the alkyl group on the 9-position of the fluorene component could be adjusted to imrove the solubility of the complexes. Three series of platinum complexes bearing fluorenyl substituent on the terdentate (C^N^N or terpyridyl) were synthesized and studied. The first series of complexes included complexes **28-38** that contained different monodentate ligand. It was discovered that the complexes with fluorenyl substituent exhibit longer triplet excited-state lifetimcs, higher emission quantum yields, and increased ratios of the excited-state absorption cross-section to that of the ground-state in comparison to those of the complexes without the

fluorenyl substituent. The complexes with chloride co-ligand (**28** and **29**) exhibit very large ratios of σ_{ex}/σ_0 due to the reduced ground-state absorption in the visible to the near-IR region. Most importantly, Complex **29** exhibit moderate two-photon absorption from 740 nm to 950 nm. Therefore, significant transmission decrease due to the two-photon induced excited-state absorption was observed in this region. Complex **29** was provided to the ARL for further study based on its broadband nonlinear absorption and good solubility in CH_2Cl_2 (~140 mg/mL). Similar to that observed for complexes in Series 4, when the electron-donating ability of the monodentate ligand increased, the low-energy charge-transfer absorption band red-shifted, which resulted in reduced ratio of σ_{ex}/σ_0 and consequently reduced reverse saturable absorption at 532 nm. The dinuclear complexes also reduced the reverse saturable absorption. The details of these studies were reported in publications #1 and 2. The key photophysical parameters and spectra are provided in Tables 2 and 3, and in Figure 2.

Series 5

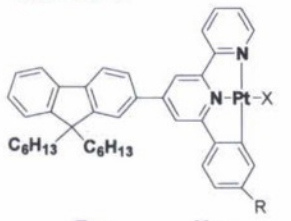

	R =	X =
28	H	Cl
29	OC_8H_{17}	Cl
30	H	$\equiv C_3H_7$
31	H	$\equiv$Ph

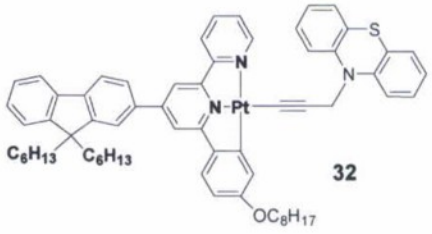

32

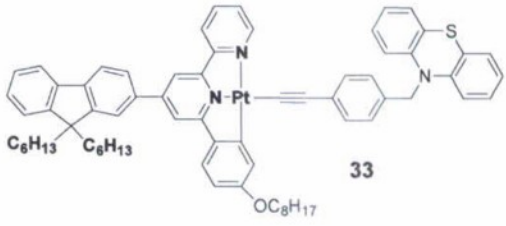

33

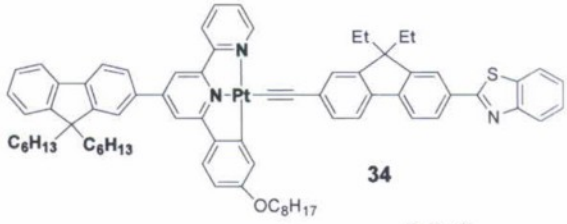

34

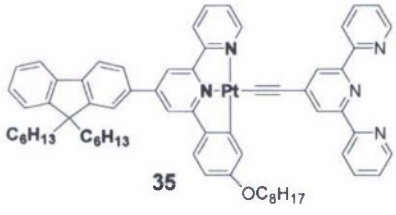

35

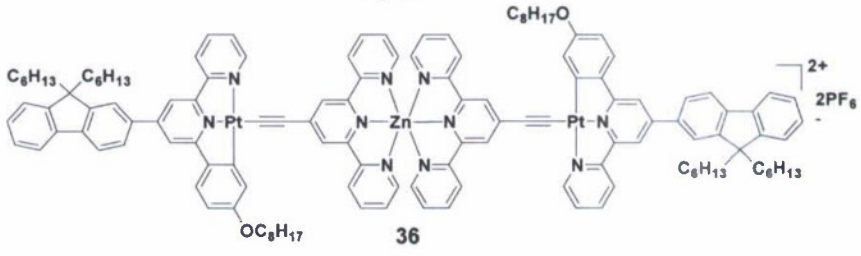

36

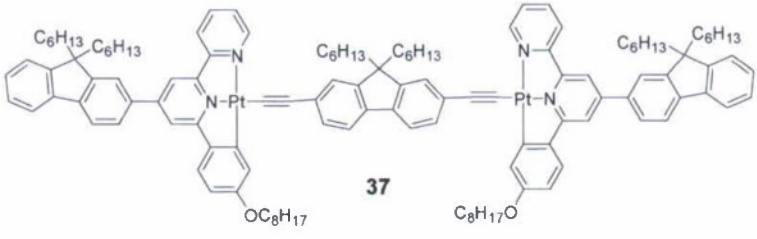

37

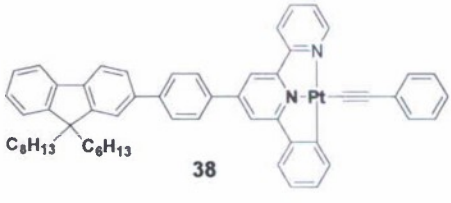

38

Table 2. Photophysical parameters of **28 – 31** and **37**.

	CH_2Cl_2[a]			CH_3CN[a]		C_3H_7CN[b]
	λ_{abs}[c]/ nm ($\varepsilon/10^3$ L·mol^{-1}·cm^{-1})	λ_{em}[c]/nm (τ_0/ns; Φ_{em})	k_Q[d] / 10^9 L·mol^{-1}·s^{-1}	λ_{em}[c]/ nm (τ_{em}/ ns, Φ_{em})	$\lambda_{T1\text{-}Tn}$/ nm (τ_{TA}/ ns; $\varepsilon_{T1\text{-}Tn}$/L·mol^{-1} ·cm^{-1}; Φ_T)	λ_{em}[c]/nm (τ_{em}/μs)
28	282 (38.2), 312 (25.9), 336 (29.6), 354 (32.3), 421 (8.6), 439 (8.8)	568 (960; 0.075)	1.63	566 (190; 0.067)	387 (140; 9070), 656 (210; 4980; 0.08)	548 (23.2), 588 (23.9), 635
29	291 (37.5), 323 (30.8), 354 (38.1), 419 (7.7), 439 (6.8)	591 (950; 0.047)	1.12	588 (570; 0.042)	475 (620; 5500; 0.16), 665 (680; 4820), 800 (480)	542(16.0), 586 (15.5),
30	288 (37.7), 339 (35.7), 355 (30.8), 443 (9.2), 463 (8.8), 529 (1.0)	593 (680; 0.073)	1.41	590 (510; 0.065)	400 (670; 11480), 635 (660; 3790; 0.11)	550 (14.0), 590 (14.2)
31	284 (48.2), 341 (31.9), 355 (30.9), 441 (10.3), 465 (9.2), 530 (1.2)	593(980; 0.076)	1.37	592 (758; 0.067)	400 (880; 11000), 645 (800; 1670; 0.24)	554 (14.0), 584 (14.5)
37	293 (80.4), 324 (79.6), 361 (126.0), 441 (24.4), 486 (24.6), 510 (22.3)	602[e] (890 (97%), 30 (3%)); 0.015)	1.94	607[g] (825 (94%), 20 (6%)); 0.008[h])	---[j]	588 (16.0), 629 (14.7)

[a] Measured at room temperature. [b] In butyronitrile glassy solutions at 77 K. [c] At a concentration of 5×10^{-5} mol/L. [d] Self-quenching rate constant. [e] At a concentration of 5×10^{-6} mol/L. [g] At a concentration of 5×10^{-6} mol/L in acetone. [h] In acetone solution. [j] Too weak to be measured.

Table 3. Excited-state absorption cross-sections of **28 – 31** in CH_2Cl_2 at 532 nm.

	σ_0[a] (10^{-18} cm^2)	σ_S[b] (10^{-18} cm^2)	σ_T[c] (10^{-18} cm^2)	σ_S/σ_0	σ_T/σ_0	$\Phi\sigma_T/\sigma_0$
28	0.765	62 ± 2	245 ± 5	81	320	25.6
29	0.536	80 ± 3	103 ± 3	149	192	30.8
30	3.29	130 ± 5	145 ± 5	40	44	4.8
31	4.21	100 ± 5	75 ± 5	24	18	4.3
76	1.60	19 ± 1	46 ± 2	12	29	14.7

[a] Ground-state absorption cross-section. [b] Singlet excited-state absorption cross-section. [c] Triplet excited-state absorption cross-section.

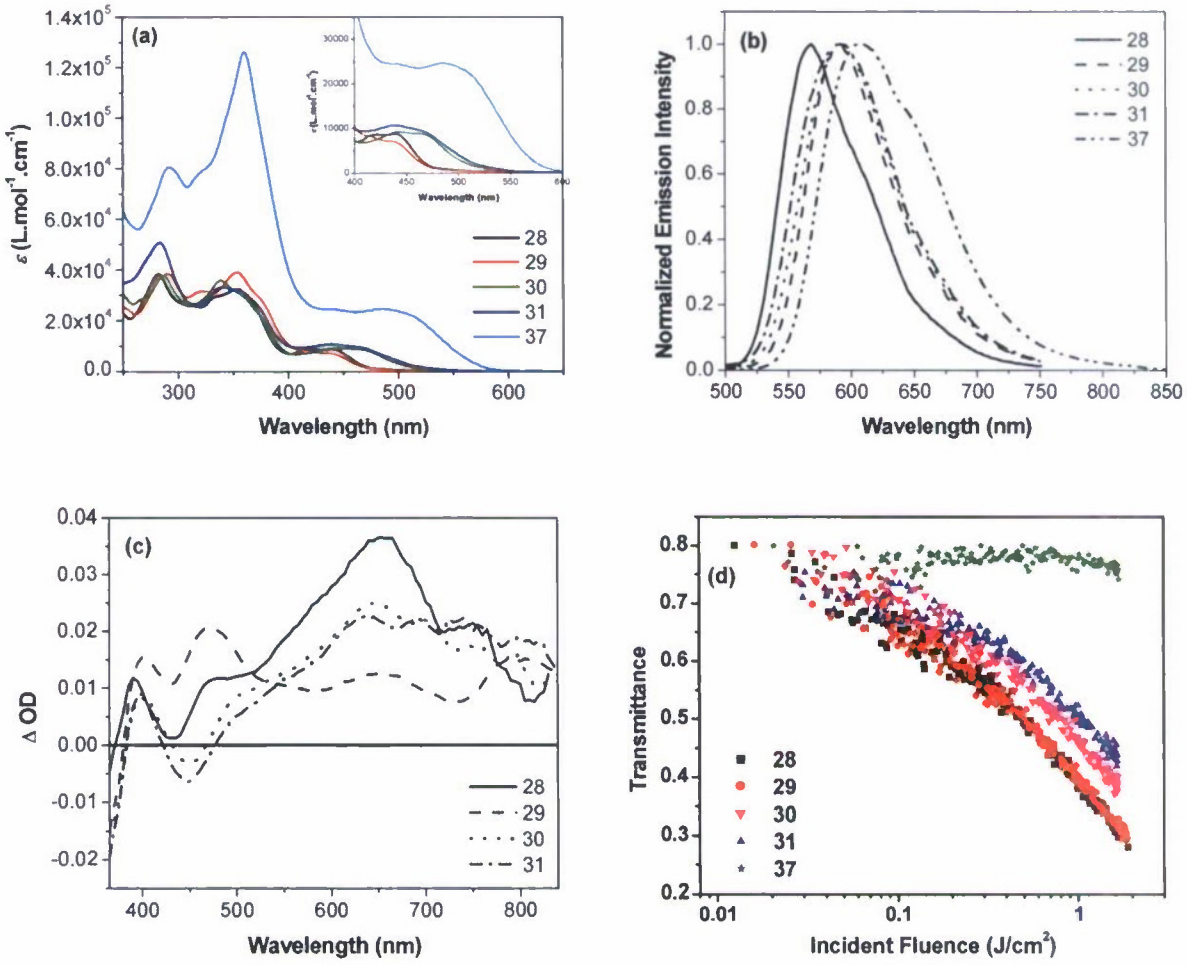

Figure 2. (a) UV-vis absorption spectra in CH_2Cl_2, (b) emission spectra in CH_2Cl_2 at room temperature, (c) ns transient difference absorption spectra in CH_3CN, (d) nonlinear transmission at 532 nm for ns laser pulses in a 2-mm cell in CH_2Cl_2 for **28-31** and **37**.

Our second approach was to introduce moderate electron-donating substituent (such as fluorenyl in complexes **39** and **40** in Serics 6) on the acetylide ligand in order to red-shift the ^{1}MLCT absorption band while maintain the broadband excited-state absorption. However, in contrast to the effect of fluorenyl substituent on the terdentate ligand, introducing the fluorenyl substituent on the acetylide ligand (complexes **39**, **40**, **41**, **44**) caused red-shift of the charge transfer band and thus reduced the ratio of σ_{ex}/σ_0, which decreased the reverse saturable absorption of the complexes.

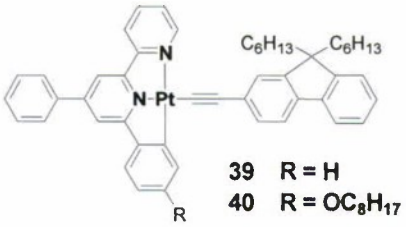

39 R = H
40 R = OC_8H_{17}

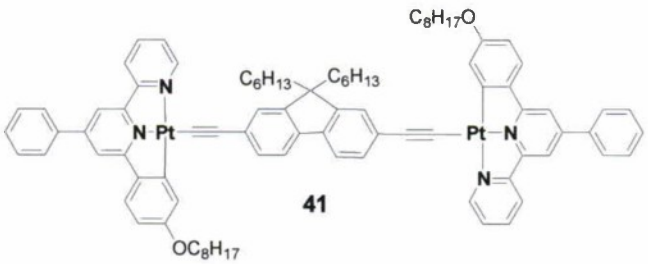

41

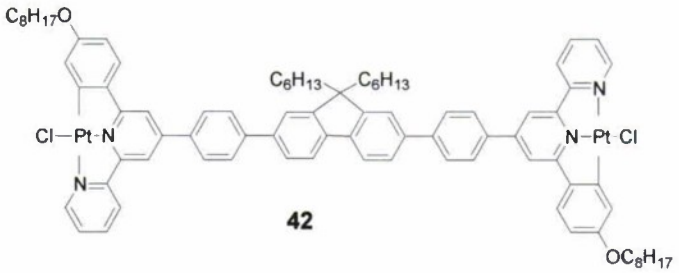

42

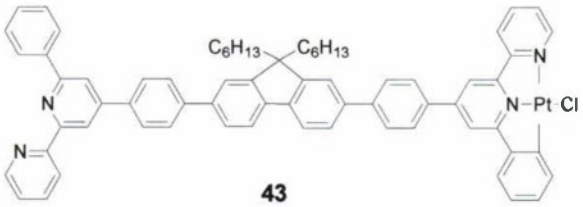

43

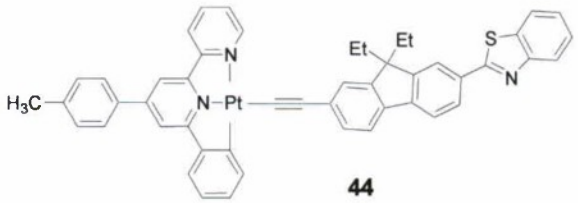

44

Series 6

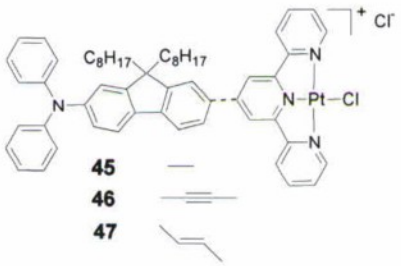

45
46
47

Series 7

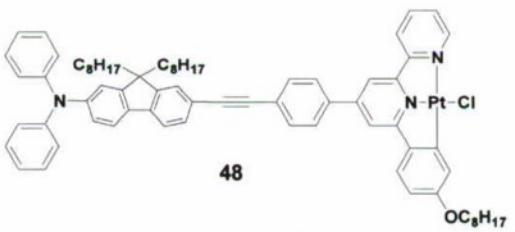

48

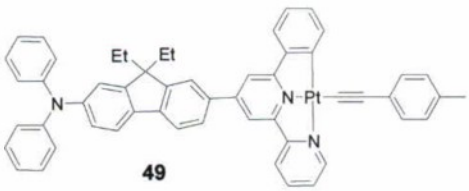

49

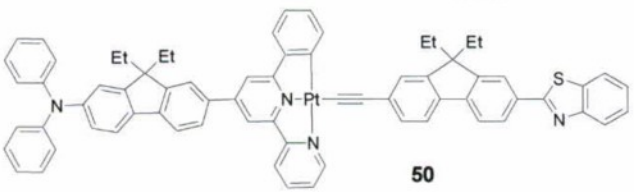

50

To further improve the two-photon absorption in the near-IR region, electron-donating diphenylamino substituent was introduced on the 7-position of the fluorenyl component (complexes **45** - **50** in Series 7). The effect of the bridging group between the diphenylaminofluorenyl component and the electron-withdrawing platinum terpyridyl chloride component was also investigated. The two-photon absorption cross-section values (σ_2) for the complexes **45** and **47** were measured to be 600 - 2000 GM by Z-scan experiment from 740 nm to 825 nm, with the largest σ_2 value to be 2000 GM at 800 nm for **47**. To the best of our knowledge, these values are the largest σ_2 values reported for platinum complexes to date. Complex **47** with the ethynylene-linker shows much stronger 2PA than complex **46** with the vinylene-linker. The

photophysical and nonlinear absorption studies for complexes **45** – **47** were reported in publication #5. The key parameters and spectra are provided in Tables 4 and 5 and in Figure 3.

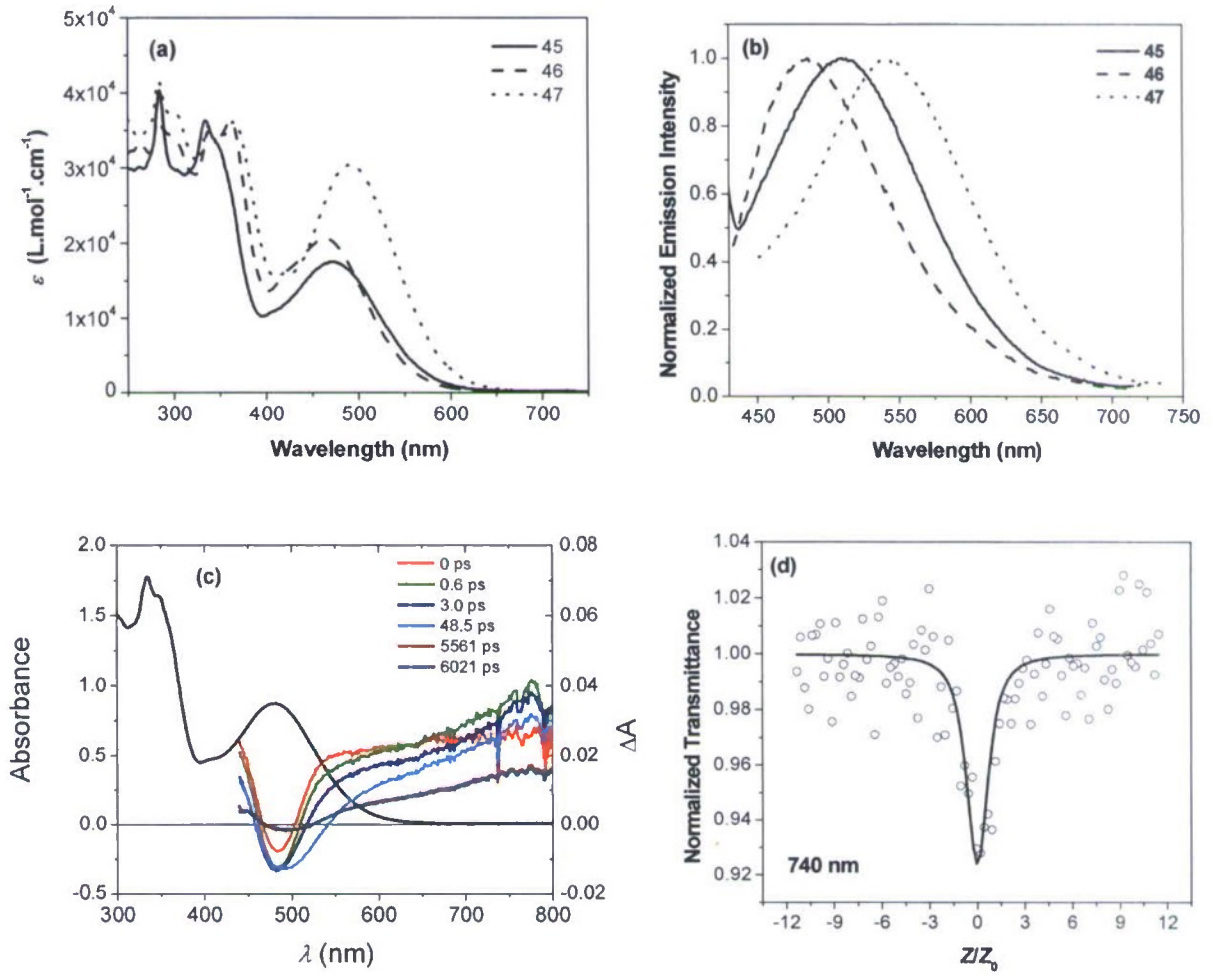

Figure 3. (a) UV-vis absorption spectra in CH_3CN for **45** - **47**, (b) Normalized emission spectra of **45** (λ_{ex} = 384 nm), **46** (λ_{ex} = 374 nm), and **47** (λ_{ex} = 389 nm) in CH_3CN at room temperature (c = 1×10^{-5} mol/L), (c) Time-resolved fs transient difference absorption spectra of **45** in CH_3CN, (d) Open-aperture Z-scan experimental data and fitting curves for **46** in CH_3CN at 740 nm

Table 4. Electronic absorption and emission data for **45**, **46**, and **47**.

	λ_{abs} /nm ($\varepsilon/10^4$ L.mol^{-1}.cm^{-1})[a]	λ_{em}/ nm (τ)[b] R.T.	Φ_{em}[c] R.T.
45	284 (4.03), 334 (3.63), 471 (1.75)	515 (48 ps (29%), 2241 ps (71%))	0.00047
46	283 (3.64), 338 (3.49), 361 (3.63), 466 (2.06)	486 (86 ps (2%), 3686 ps (98%))	0.00035
47	284 (4.16), 338 (3.55), 365 (3.61), 492 (3.04)	532 (150 ps (8%), 2976 ps (92%))	0.00019

[a] Electronic absorption band maxima and molar extinction coefficients in CH_3CN, $c \approx 1\times10^{-5}$ mol/L. [b] The emission band maxima and decay lifetimes measured in CH_3CN solutions. λ_{ex} =

375 nm. [c] Emission quantum yield measured at λ_{ex} = 436 nm with A_{436} = 0.1 in CH_3CN solution. $[Ru(bpy)_3]Cl_2$ was used as the reference.

Table 5. Excited-state absorption and two-photon absorption cross-sections for **45-47** at different wavelengths.

Complex	λ (nm)	σ_0 (10^{-18} cm^2)[a]	σ_S (10^{-18} cm^2)[b]	σ_S/σ_0	σ_2 (GM)
45	575	10.1	20±1	2.0	
	600	3.83	20±2	5.2	
	630	0.956	17±1	18	
	670	0.191	25±1	131	
	740		24.4[c]		850±50
46	550	14.7	38±2	2.6	
	575	6.31	24±2	3.8	
	600	2.49	24±2	9.6	
	630	0.765	26±2	34	
	680	0.153	12±1	78	
	740		7.7[c]		1200±100
	760		11.1[c]		1000±200
	800		7.7[c]		2000±200
	825		11.6[c]		600±100
47	575	25.8	43±5[d]	1.7	
	600	10.9	36±2	3.3	
	630	3.63	20±2	5.5	
	670	0.765	16±1	21	

[a] Ground-state absorption cross-section. [b] Effective singlet excited-state absorption cross-section with the assumption of $\sigma_{S2} = \sigma_S$. [c] Estimated from the fs TA data at zero time delay. [d] $\sigma_{S2} = (12\pm7)\times10^{-18}$ cm^2.

In contrast to the approaches demonstrated by complexes **45** - **50**, we designed and synthesized a series of complexes with benzothiazolylfluorenyl substituent attached on the C^N^N or terpyridyl ligand (**51** – **59** in Series 8). Different electron-donors and acceptors were introduced to the acetylide ligand in order to understand whether the A-π-A-π-A or A-π-A-π-D system exhibit stronger nonlinear absorption. It was discovered that complexes **51** – **55** exhibit relatively weak excited-state absorption in the visible to the near-IR region. The complex with nitrophenylacetylide ligand (**55**) showed the strongest nonlinear transmission at 532 nm for ns pulses among these complexes. The TPA of these complexes needs to be studied in the near future. In contrast, complexes **57** and **58** exhibit strong triplet excited-state absorption in the visible spectral region, relatively long triplet excited-state lifetime and moderate triplet excited-state quantum yield. Thus strong reverse saturable absorption was observed for these two complexes at 532 nm for ns laser pulses. In addition, these two complexes exhibit strong two-photon absorption in the near-IR region. Broadband nonlinear transmission was demonstrated for these two complexes from 480 nm to 910 nm. The spectra and photophysical data for **57** and **58** are shown in Figure 4 and Table 6.

Series 8

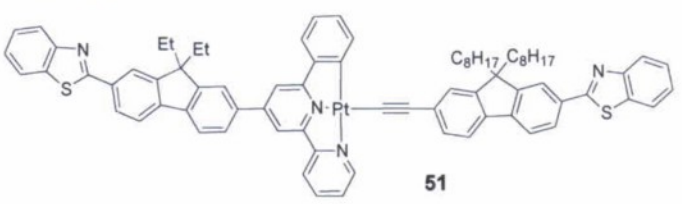

51

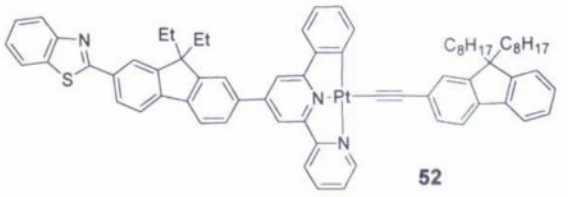

52

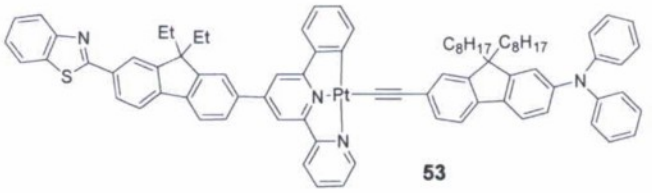

53

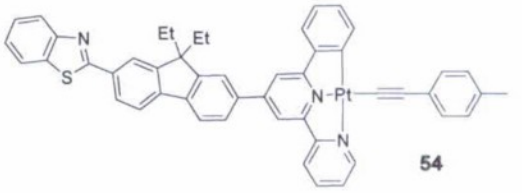

54

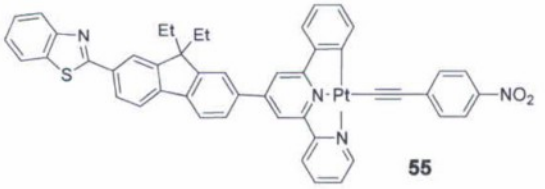

55

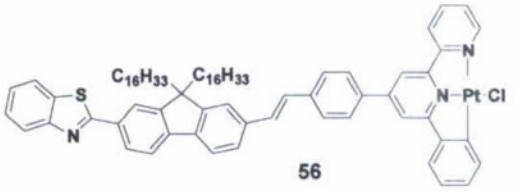

56

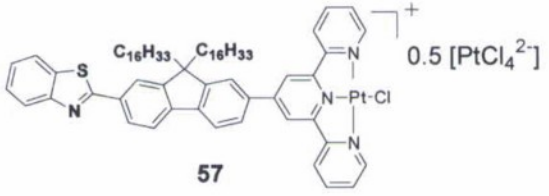

57

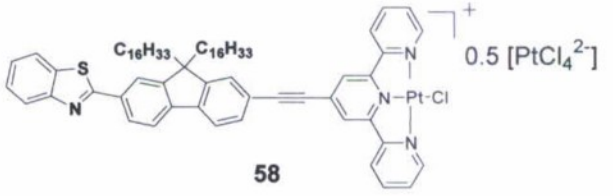

58

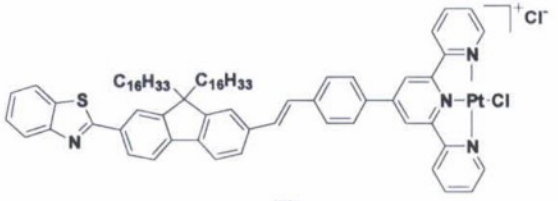

59

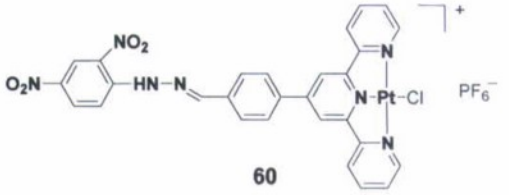

60

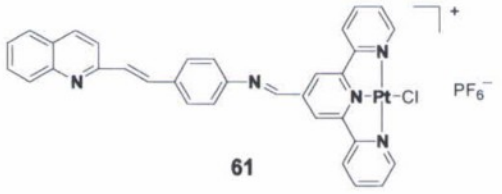

61

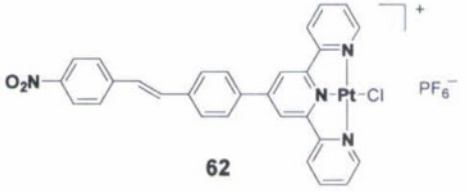

62

Because our study on complexes **21 – 27** revealed that electron-donating substituent could increase the lifetime of the triplet excited state and increase the σ_{ex}/σ_0 ratio, both of them would enhance the reverse saturable absorption. To further improve the reverse saturable absorption and to introduce TPA in the near-IR region, we synthesized complex **63**. The UV-vis and transient difference absorption spectra of **63** is shown in Figure 4. Complex **63** exhibit triplet excited-state absorption in the visible to the near-IR region and the triplet excited-state lifetime was ~4.5 μs. The nonlinear transmission of **63** for ns pulses at 532 nm was comparable to that of SiNc. Picosecond Z-scan study demonstrated that **63** exhibit broadband nonlinear transmission from 450 nm to 910 nm. Fitting of the Z-scan data resulted in the singlet and triplet excited-state absorption

cross sections in a variety of visible to the near-IR region and the TPA cross section values in the near-IR region. These data are piled in Tables 6 and 7.

Table 6. Triplet excited state parameters of **57** and **58** in CH_3CN and **63** and **65** in CH_2Cl_2

Complex	λ_{T1-Tn}/nm (ε_T/$M^{-1}.cm^{-1}$)	$\tau_T/\mu s$	Φ_T
57	530 (26770)	3.37	0.26
58	545 (39910)	1.72	0.44
63	620 (56250)	4.55	0.17
65	620 (60170)	10.78	0.14

SiNC in C_6H_6 was used as reference (ε_{590}=53400$M^{-1}cm^{-1}$, Φ_T=0.20).

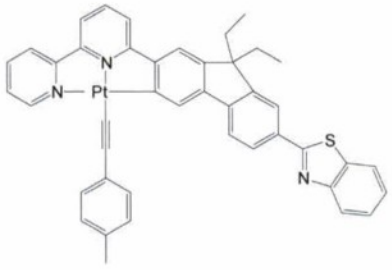

63

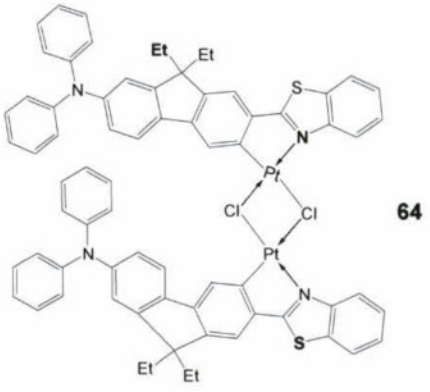

64

Table 7. Absorption cross sections of **63** in CH_2Cl_2 solution

λ/nm	**σ_0**	**σ_S[a] 10^{-18} cm^2**	**σ_T[b]**	**σ_S/σ_0**	**σ_T/σ_0**	**σ_2/GM**
430	29.6	35	133	1.2	4.5	--
475	14.3	30	158	2.1	11.0	--
500	6.75	48	173	7.1	25.6	--
532	1.48	40±5	170±10	27	115	--
550	1.25	40	191	32	153	--
575	0.344	40	256	116	744	--
600	0.0956	45	323	471	3.38×10^3	--
630	0.0318	200	420	6.29×10^3	1.32×10^4	--
680	0.01	180	245	1.80×10^4	2.45×10^4	--
740	~0	40	143	--	--	600
800	~0	27	148	--	--	650
850	~0	--	--	--	--	1200
875	~0	--	--	--	--	220
910	~0	--	--	--	--	200

[a] Effective singlet excited-state absorption cross section. [b] Effective triplet excited-state absorption cross section.

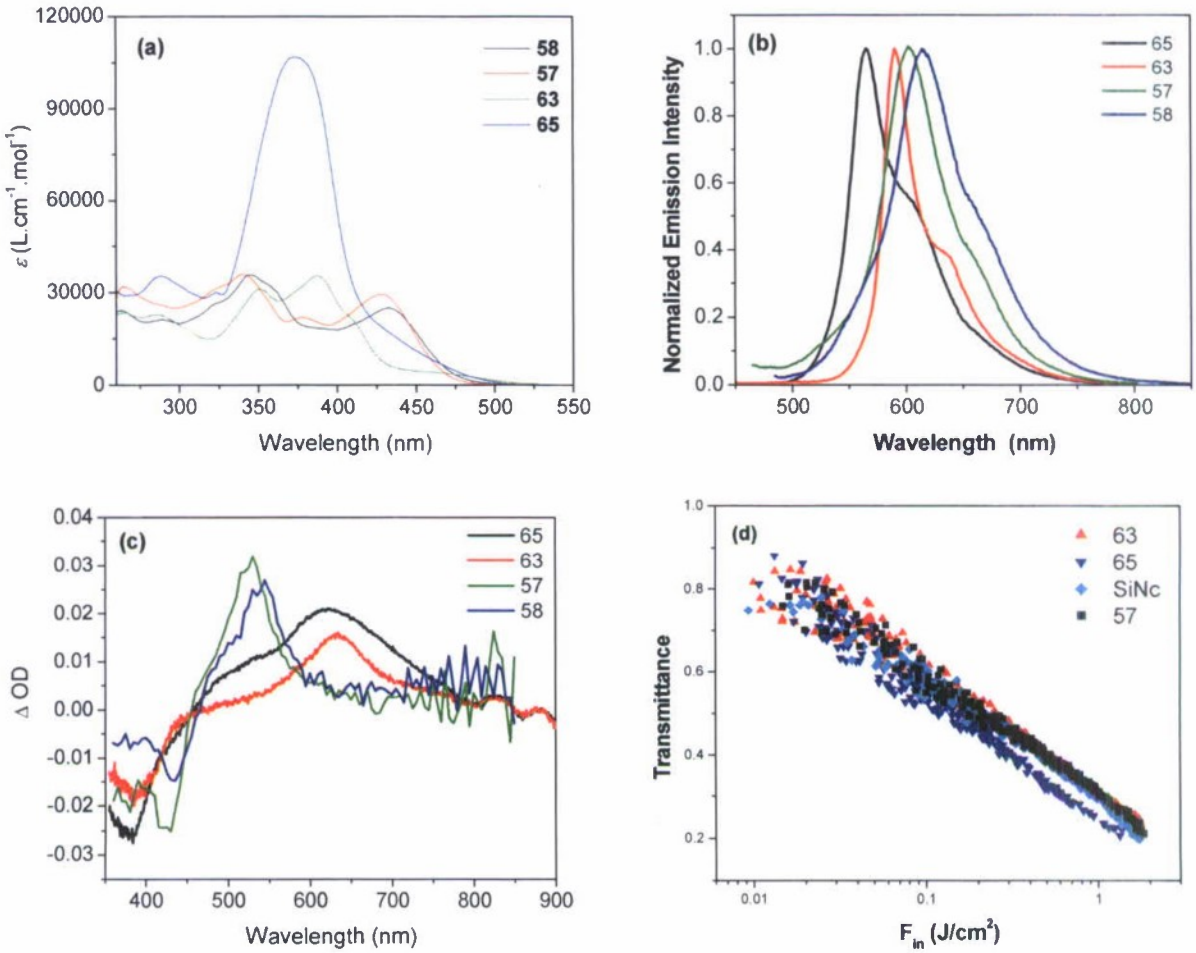

Figure 4. (a) UV-vis absorption spectra of **57**, **58**, **63** and **65** in CH_2Cl_2; (b) Normalized emission spectra of **57**, **58**, **63** and **65** in CH_2Cl_2; (c) ns transient difference absorption spectra of **57** and **58** in CH_3CN, and **63** and **65** in CH_2Cl_2 at zero delay after excitation; (d) Nonlinear transmission of **57, 63** and **65** in CH_2Cl_2 for ns laser pulses at 532 nm. T_{lin} = 80% in a 2-mm cuvette.

It was reported in the literature that some of the platinum bipyridine complexes with acetylide ligands exhibit broadband excited-state absorption. Several of our studies summarized above have demonstrated that platinum complexes with benzothiazolylfluorenyl component exhibit broadband nonlinear absorption. We anticipated that platinum bipyridine complexes with benzothiazolylfluorenyl acetylide ligands would exhibit broadband nonlinear transmission. To demonstrate this, complexes **65** – **68** were synthesized. The different alkyl chains were used to adjust the solubility of the complexes. The complex with the best solubility in CH_2Cl_2 and toluene is **67**. The UV-vis, emission, transient difference absorption spectra and the nonlinear transmission plot for complex **65** are given in Figure 4. The photophysical data and the excited-state absorption cross sections and the TPA cross sections are listed in Tables 6 and 8. The ratios of σ_{ex}/σ_0 in the visible and the TPA cross sections in the near-IR region for complex 65 are among the largest values reported for organometallic complexes. The details of the photophysical study and nonlinear absorption of **65** have been reported in our publications #3 and #6. The photophysical parameters and the nonlinear absorption of complexes **66-68** are similar to those for complex **65**. The nonlinear absorption of **69** and **70** is much weaker than those of **65-68**.

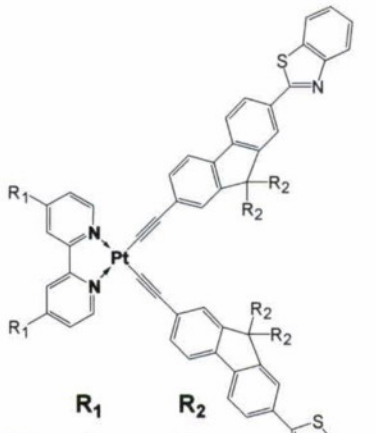

	R_1	R_2
65	*t*-Bu	Et
66	C_9H_{19}	$C_{16}H_{33}$
67	$C_{17}H_{35}$	$C_{16}H_{33}$
68	$C_{17}H_{35}$	C_8H_{17}

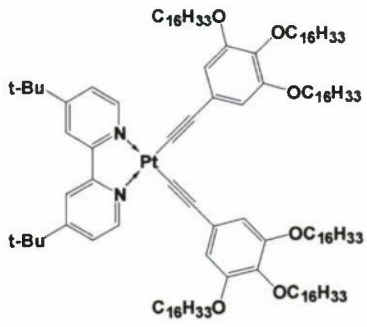

69

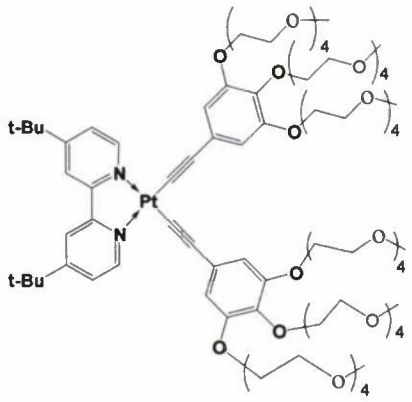

70

Table 8. Absorption cross sections of **65** in CH_2Cl_2 solution[a]

λ nm	σ_0[b]	σ_{S1}[c]	σ_T[d]	σ_{S2}[e]	σ_{S1}/σ_0	σ_T/σ_0	σ_{S2}/σ_0	σ_2[f]
		10^{-18} cm^2						GM
450	39.4	35	94[h]	120	0.89	2.4	3.0	--
475	21.2	46	250[h]	70	2.2	11.8	3.3	--
500	5.55	48	375[h]	70	8.6	67.6	12.6	--
532	0.383	60	460	70	157	1.20×10^3	183	--
550	0.0765	75	550[h]	70	980	7.19×10^3	915	--
575	0.0188	95	760[h]	350	5.05×10^3	4.04×10^4	1.86×10^4	--
600	0.0084	110	900[h]	1000	1.31×10^4	1.07×10^5	1.19×10^5	
630	~0	100[g]	870[h]	30	--	--	--	1000
680	~0	70[g]	650[h]	30	--	--	--	400
740	~0	40[g]	400[h]	10	--	--	--	600
760	~0	34[g]	285[h]	10	--	--	--	1000
800	~0	28[g]	320[h]	10	--	--	--	300
825	~0	28[g]	240[h]	1	--	--	--	80
850	~0	--	--	--	--	--	--	600[i]
875	~0	--	--	--	--	--	--	300[i]
900	~0	--	--	--	--	--	--	300[i]

[a] Determined by fitting Z-scan data except where otherwise indicated. [b] The ground-state absorption cross section. [c] The first singlet excited-state absorption cross section. [d] The effective triplet excited-state absorption. [e] The second singlet excited-state absorption cross section. [f] The two-photon absorption cross section. [g] Determined from the value $\sigma_S(532\text{ nm}) = 6\times10^{-17}$ cm^2 and the fs transient difference absorption spectrum at 0 time delay. [h] $\sigma_T(532\text{nm}) = 4.6\times10^{-16}$ cm^2 determined from combined fitting of ns and ps *Z*-scan data. For other wavelength, $\sigma_T(\lambda)$ is determined from the value of $\sigma_T(532\text{nm})$ and the fs transient difference absorption spectrum at 5.8-ns time delay. [i] Effective cross-section for excited-state-assisted two-photon absorption.

In order to obtain liquid Pt(II) complexes, we synthesized complexes **71** and **72** with multiple polyether chains and long alkyl chains. The photophysics and nonlinear absorption of these two complexes were investigated and the results are shown in Figure 5 and Table 9. Both complexes exhibit RSA and/or TPA from 450 nm to 825 nm for ps laser pulses. Both of them are viscose liquid/solid.

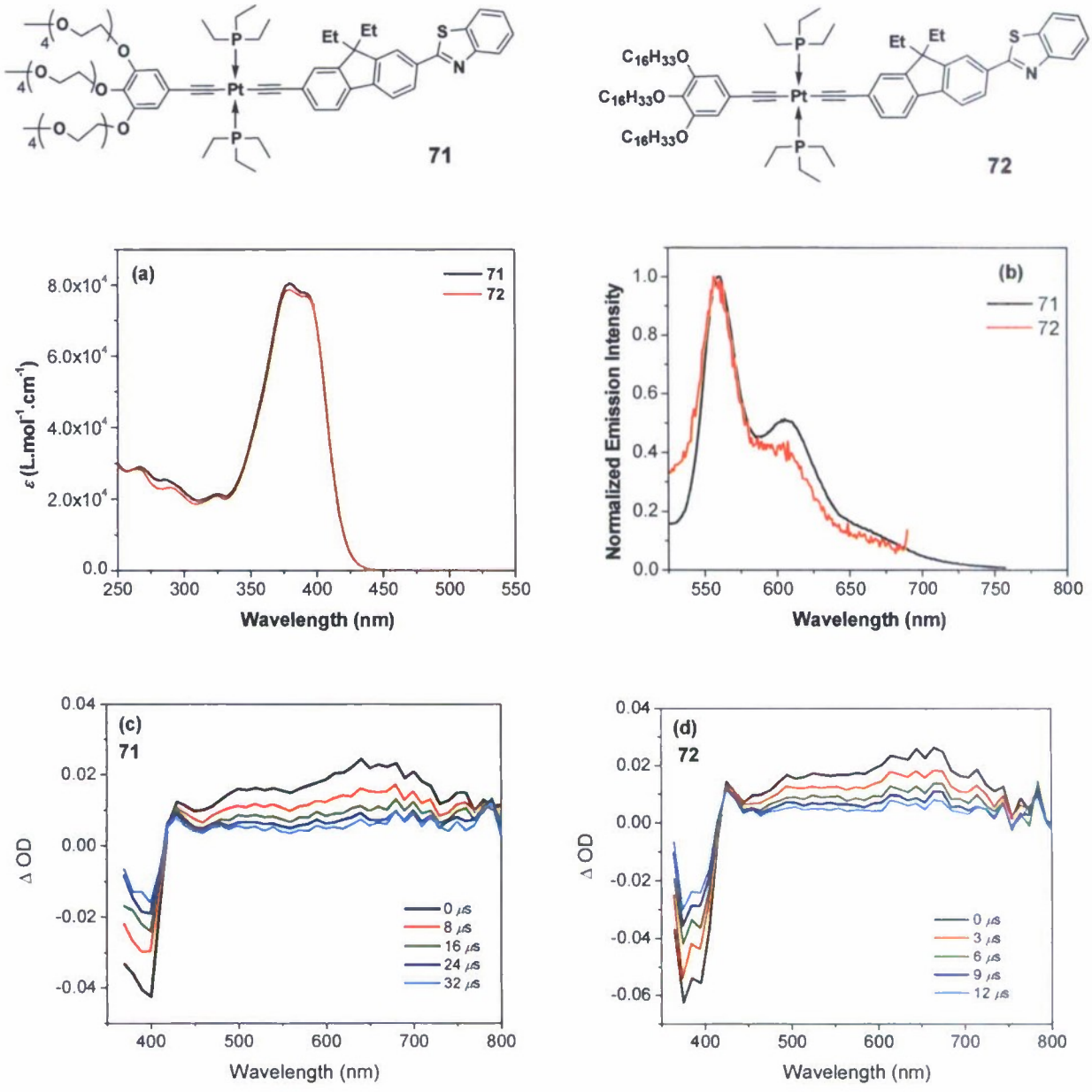

Figure 5. (a) UV-vis absorption spectra of **71** and **72** in CH_2Cl_2; (b) Normalized emission spectra of **71** and **72** in CH_2Cl_2; (c) Time-resolved ns transient difference absorption spectra of **71** in CH_2Cl_2; (d) Time-resolved ns transient difference absorption spectra of **72** in CH_2Cl_2.

Table 9. Triplet excited-state parameters of **71** and **72** in CH_2Cl_2

Complex	$\lambda_{T1\text{-}Tn}$/nm (ε_T[a]/$M^{-1}.cm^{-1}$)	$\tau_T/\mu s$	Φ_T[b]
71	640 (37090)	23.4	0.31
72	635 (21690)	12.9	0.49

[a] Measured using the singlet depletion method. [b] SiNc in benzene was used as the reference (ε_{590}=53400$M^{-1}cm^{-1}$, Φ_T=0.20).

The photophysics and nonlinear absorption of complexes **73** – **76** were investigated. Complexes **73**, **74** and **76** exhibit strong RSA at 532 nm. However, due to the limited solubility of these complexes in organic solvents, they are not ideal candidates as broadband nonlinear absorbing materials. The details of the photophysics and nonlinear absorption of complexes **74** and **76** are published in papers #16 and 18.

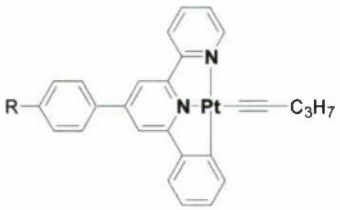

73 R = Br; **74** R = H

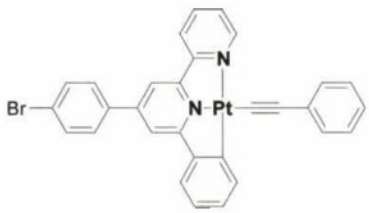

75

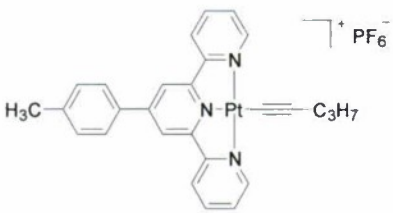

76

In order to understand how the intramolecular interactions influence the photophysics and nonlinear absorption of Pt(II) complexes, a dinuclear Pt(C^N^N) complex (**77**) and a trinuclear complex (**78**) were synthesized and investigated. Complex **77** exhibit weak ground-state absorption in the visible to the near-IR region; but strong excited-state absorption in this region. Therefore, strong RSA was observed at 532 nm for ns laser pulses. The RSA of **77** is even stronger than that of SiNc. The photophysical parameters and the spectra for **77** are given in Table 10 and in Figure 6.

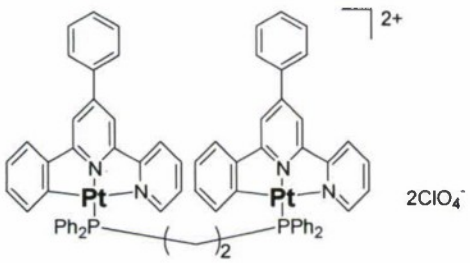

77

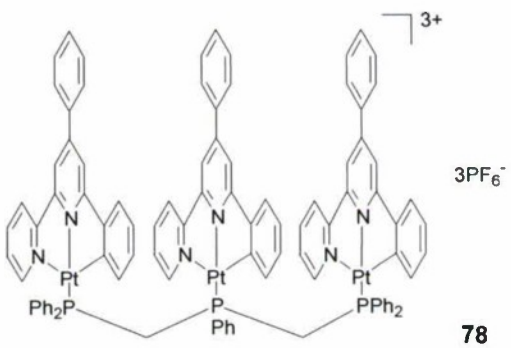

78

Table 10. Photophysical parameters for complex **77** in acetonitrile

Complex	UV-vis[a] λ_{max}/nm (ε/dm^{3}mol^{-1}cm^{-1})	Emission[a] λ_{max}/nm (τ/ns) 298 K	Emission[a] λ_{max}/nm (τ/ns) 77 K	TA[b] λ_{max}/nm (τ/ns) 298 K
77	287 (53900), 356 (16500), 427 (1300), 510 (110)	544 (1497); 591 (1476)	534 (3409, 92%; 313, 8%); 581 (3456, 94%; 271, 6%)	385 (1822); 571 (1784)

[a] Measured at a complex concentration of 1.2×10^{-4} mol/L for **1**, 1.4×10^{-4} mol/L for **2**, and 1.3×10^{-4} mol/L for **3**. [b] Complex concentration is 2.7×10^{-5} mol/L for **1**, 3.2×10^{-5} mol/L for **2**, and 1.9×10^{-5} mol/L for **3**.

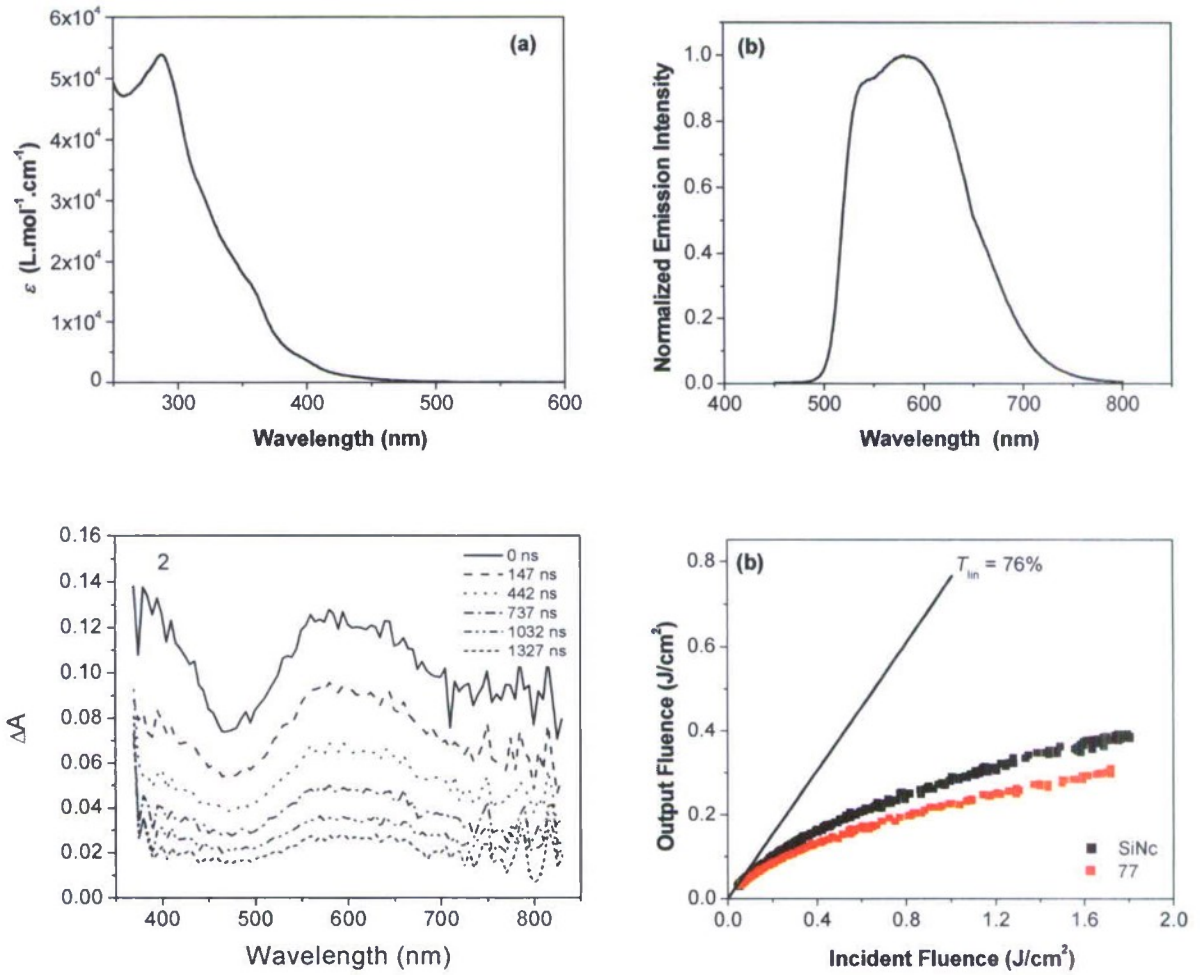

Figure 6. (a) UV-vis absorption spectra of **77** CH_3CN ($c = 1.4\times10^{-4}$ mol/L); (b) Normalized emission spectra of **77** in CH_3CN ($c = 1.4\times10^{-4}$ mol/L); (c) Time-resolved ns transient difference absorption spectra of **77** in CH_3CN; (d) Nonlinear absorption of **77** for ns laser pulses at 532 nm in a 2-mm cell.

For the trinuclear complex **78**, the intramolecular Pt-Pt interactions red-shift the lowest absorption band to 600 nm. It exhibits broad, positive and strong transient difference absorption bands from near UV extending to near-IR spectral region (400 – 750 nm). However, due to the increased ground-state absorption in the visible region, the nonlinear transmission performance of complex **78** decreases at 532 nm. In comparison to its corresponding mononuclear complex (C^N^N)PtPPh$_3$ and the dinuclear complex [(C^N^N)Pt]$_2$dppm, the ratios of σ_{ex}/σ_0 for **78** at each respective wavelength is smaller than those of its corresponding mononuclear and dinuclear complexes. The details of the photophysical study and nonlinear absorption of complex **78** are reported in publications #13 and 21. The key photophysical parameters and the excited-state absorption cross sections are shown in Tables 11 and 12.

Table 11. Photophysical parameters of (C^N^N)PtPPh$_3$, [(C^N^N)Pt]$_2$dppm, and **78** in CH_3CN.

	τ_S / ps	τ_T / ns	Φ_T	$\lambda_{T1\text{-}Tn}$/nm ($\varepsilon_{T1\text{-}Tn}$/l.mol^{-1}.cm^{-1})	τ_{isc}/ps[a]
(C^N^N)PtPPh$_3$	8.9± 1.7	127± 3	0.23	540 (4292)	38.7
[(C^N^N)Pt]$_2$dppm	3.2± 1.0	184±9	0.25	590 (3100)	12.8
78	8.9± 2.8	588±23	0.12	600 (6240)	74.2

[a] $\tau_{isc} = \tau_s/\Phi_T$

Table 12. Wavelength-dispersion of excited-state absorption cross-sections of (C^N^N)PtPPh$_3$, [(C^N^N)Pt]$_2$dppm, and **78** in CH_3CN

	λ/nm	σ_g/10^{-19} cm^2	σ_s/10^{-18} cm^2	σ_s/σ_g	σ_T/10^{-18} cm^2	σ_T/σ_g
(C^N^N)PtPPh$_3$	475	2.68	60	224	6.0	22.4
	500	1.45	40	276	6.2	42.8
	532	0.22	60	2727	6.5	295
	550	0.15	110	7333	7.0	467
[(C^N^N)Pt]$_2$dppm	532	20.3	1	0.50	50	24.6
	550	7.20	45	62.5	60	83.3
	570	3.40	70	206	69	203
78	532	64.7	--	--	30	4.64
	550	43.7	18	4.12	45	10.3
	570	21.6	35	16.2	58	26.9
	600	12.8	40	31.3	68	53.1

In order to access the effect of different terdentate ligands on the nonlinear absorption, we synthesized the Pt(II) complexes **79** – **87**. Except for complex **82** that exhibits moderate RSA at 532 nm for ns laser pulses, the rest of the complexes all exhibit weak or no excited-state absorption and thus weak or no RSA at 532 nm.

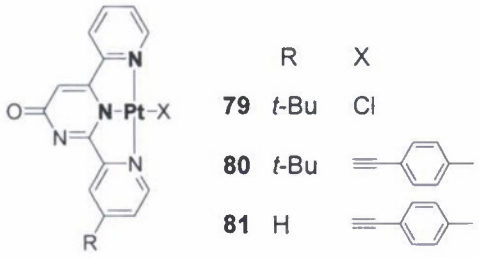

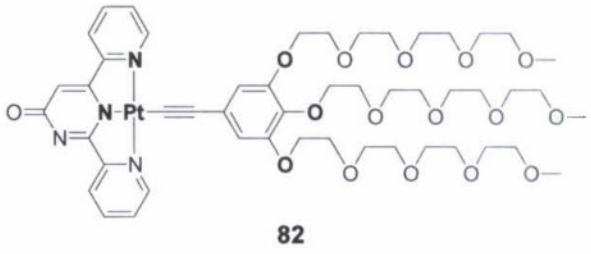

82

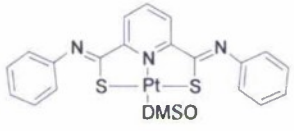

83

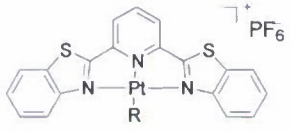

R = Cl 84

Ph 85

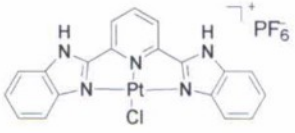

86

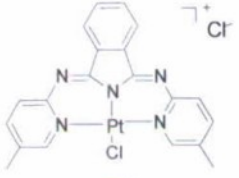

87

A.2. Photophysical and nonlinear absorption studies of Pt(II) C^N^N complexes with different acetylide ligands

In addition to the Pt(II) complexes we synthesized (complexes **1** – **87**), we also investigated the photophysics and nonlinear absorption of a series of Pt(II) C^N^N complexes with difference acetylide ligands (complexes **1a** – **1k,** which were synthesized by Prof. Hongjun Zhu's group in Nanjing University of Technology in China). The UV-vis spectra, ns transient difference absorption spectra and the nonlinear transmission curves are provided in Figure 7 and the photophysical parameters are listed in Table 13. Except for **1d**, **1g**, **1h, 1i** and **1j**, all of the other complexes exhibit broad and relatively strong triplet excited-state absorption in the visible extending to the near-IR region. Most of the complexes exhibit reverse saturable absorption for ns laser pulses at 532 nm, with the RSA strength decreasing following this trend: **1k≈1a>1c>1f≈1i>1h≈1b>1e>1d>1g**, which was mainly determined by the ratio of the triplet excited-state absorption cross section to that of the ground-state and the triplet excited-state quantum yield. Introducing electron-withdrawing substituent or extending the conjugation length of the acetylide ligand could reduce the ground-state absorption cross section while increasing the triplet excited-state absorption cross section. Consequently, the RSA for these complexes is improved. The details of this work were reported in publication #7.

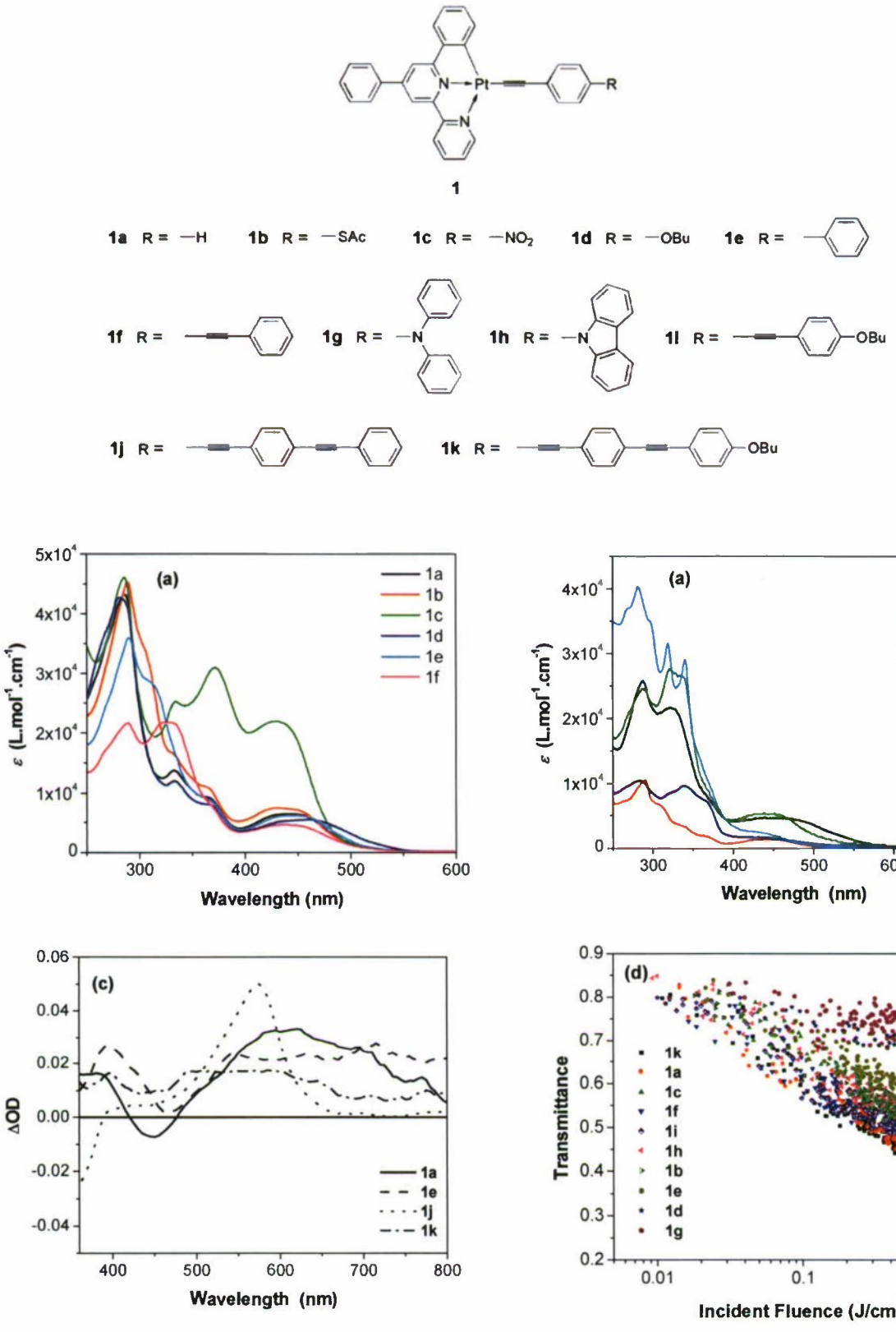

Figure 7. (a) UV-vis absorption spectra of **1a – 1k** in CH_3CN; (b) ns transient difference absorption spectra of **1a – 1k** in CH_3CN at zero delay after laser excitation; (c) Nonlinear absorption of **1a – 1k** in CH_2Cl_2 solution for ns laser pulses at 532 nm in a 2-mm cell.

Table 13. Photophysical parameters of **1a-1k** in CH_3CN[a]

	λ_{abs}[b]/nm ($\varepsilon/10^3$ L·mol^{-1}·cm^{-1})	λ_{em}[b]/nm (τ_{em}/ns, Φ_{em})	$\lambda_{T1\text{-}Tn}$/nm (τ_{TA}/ns; $\varepsilon_{T1\text{-}Tn}$/L·mol^{-1}·cm^{-1}; Φ_T)
1a	285 (43.2), 332 (13.8), 365 (9.4), 432 (6.36), 450 (6.42)	584 (500, 0.048)	615 (510, 3004, 0.41)
1b	289 (45.2), 332 (16.6), 365 (10.8), 429 (7.42), 448 (7.09)	570 (360,0.073)	615 (490, 10455, 0.18)
1c	286 (50.0), 332 (25.2), 372 (31.0), 432 (22.1)	555 (380, 0.024)	610 (400, 9305, 0.16)
1d	281 (42.7), 333 (12.0), 367 (8.0), 440 (5.18), 466 (5.40)	584 (90, 0.001)	[c]
1e	290 (36.0), 366 (9.0), 436 (6.14), 455 (6.08)	592 (250, 0.018)	540 (450, 2422, 0.13)
1f	289 (21.6), 327 (21.7), 422 (4.50), 440 (4.57)	582 (410, 0.062)	605 (840, 15873, 0.08)
1g	287 (25.7), 322 (21.5), 437 (4.68), 472 (4.55)	601 (190, 0.003)	[c]
1h	291 (10.4), 341 (3.2), 364 (1.8), 435 (1.33), 455 (1.28)	593 (70, 0.004)	[c]
1i	287 (24.6), 332 (27.6), 430 (5.19), 453 (5.19)	568 (280, 0.015)	[c]
1j	285 (10.4), 339 (9.6), 427 (1.73)	572 (550, 0.047)	580 (15480, 2758, 0.18)
1k	282 (40.3), 319 (31.5), 340 (29.1), 430 (sh. 2.56)	569 (210, 0.021)	580 (260, 5432, 0.11)

[a] Measured at room temperature. [b] At a concentration of 5×10^{-5} mol/L. [c] Too weak to be measured.

A.3. Synthesis, photophysics and nonlinear absorption of expanded porphyrin derivatives

The PI's previous work has found that the expanded porphyrin cadmium complex **88** exhibit comparable nonlinear transmission performance to SiNc at 532 nm for both ns and ps laser pulses (W. Sun, C.C. Byeon, M.M. McKerns, C.M. Lawson, G.M. Gray, D. Wang, *Appl. Phys. Lett.* **73**(9), 1167 (1998)). However, the photophysical properties have not been fully explored. Therefore, during this project we re-synthesized this complex and systematically investigated the emission and transient absorption spectra, as well as the triplet absorption coefficient and triplet excited state quantum yield. This complex exhibits a positive transient absorption band from 480 nm to 550 nm (Figure 8). Although the quantum yield of the formation of triplet excited state is low (Φ_T = 0.02), this complex possesses a very large triplet excited-state absorption coefficient (ε_T^{490nm} = 22,760 M^{-1}·cm^{-1}) and long triplet excited state lifetime (τ_T = 10.5 μs), which leads to the strong nonlinear transmission for ns laser pulses. In addition, ns Z-scan measurement has revealed that this complex exhibits a self-defocusing effect at 532 nm in addition to its strong reverse saturable absorption at this wavelength.

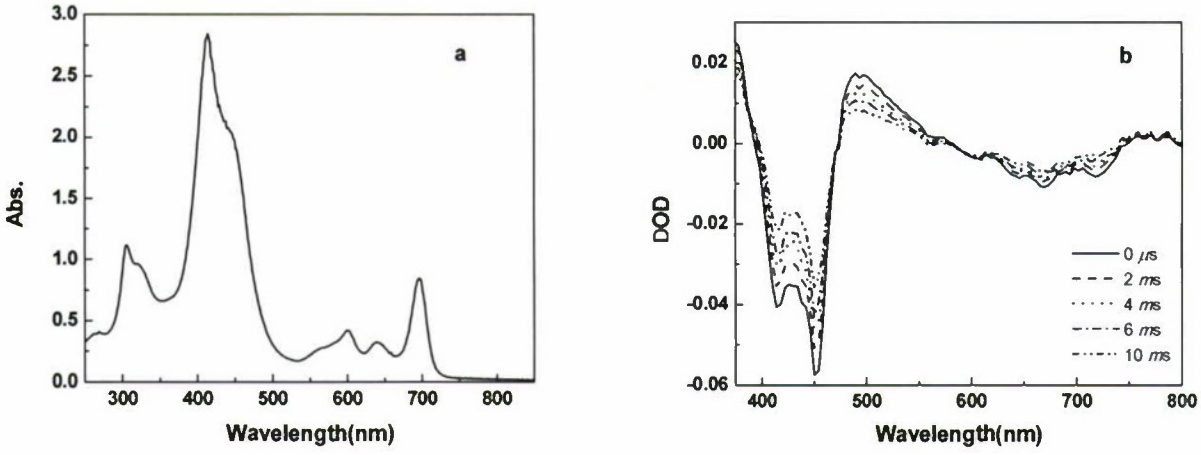

Figure 8. UV-vis absorption spectrum (a) and time-resolved triplet transient difference absorption spectra of complex **88** in a 1-cm cell in methanol.

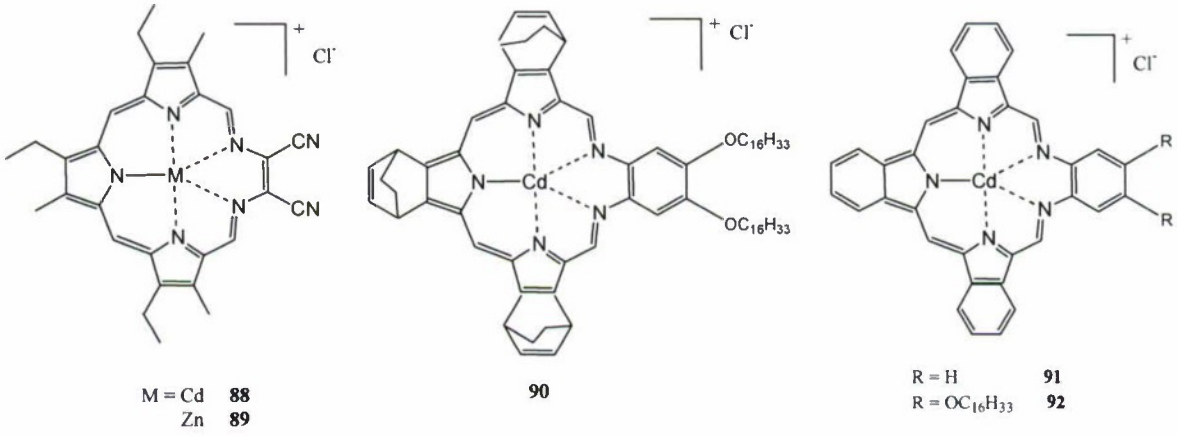

To evaluate the effect of central metal and the effect of extensive π-conjugation and electron delocalization on the photophysics and nonlinear transmission, complexes **89** – **92** were synthesized. The photophysical properties and the nonlinear transmission behavior of complexes **90** and **92** were systematically investigated. As shown in Figure 9 and Table 14, complex **92**, which is fully conjugated with the bezene rings, exhibit significant bathochromic shifts for both the B-band abd the Q-band (86 nm) in its UV-vis absorption spectrum in comparison to its precusor, complex **90**. The triplet transient difference absorption spectra of **90** and **92** display two bleaching bands that correspond to the B-band and Q-band in the UV-vis absorption spectra, respectively, and a positive band at 490 nm for **90** and 520 nm for **92**. The triplet excited state lifetimes of both complexes are quite long, ~2 μs, and the quantum yield of triplet excited state formation is relatively high, 0.56 for **90** and 0.78 for **92**. However, although **90** and **92** exhibit relatively long triplet lifetimes and high yields of triplet excited state formation, their triplet excited-state absorption cross-sections at 532 nm are relatively small. On the other hand, their ground-state absorption cross-sections at 532 nm are relatively high. Therefore, the ratio of σ_{ex}/σ_g is small, which results in weak nonlinear transmission, as shown in Figure 10. The much weaker

nonlinear transmission of **92** should be related to its higher ground-state absorption cross-section at 532 nm. The detailed study for **90** and **92** was reported in publication #14.

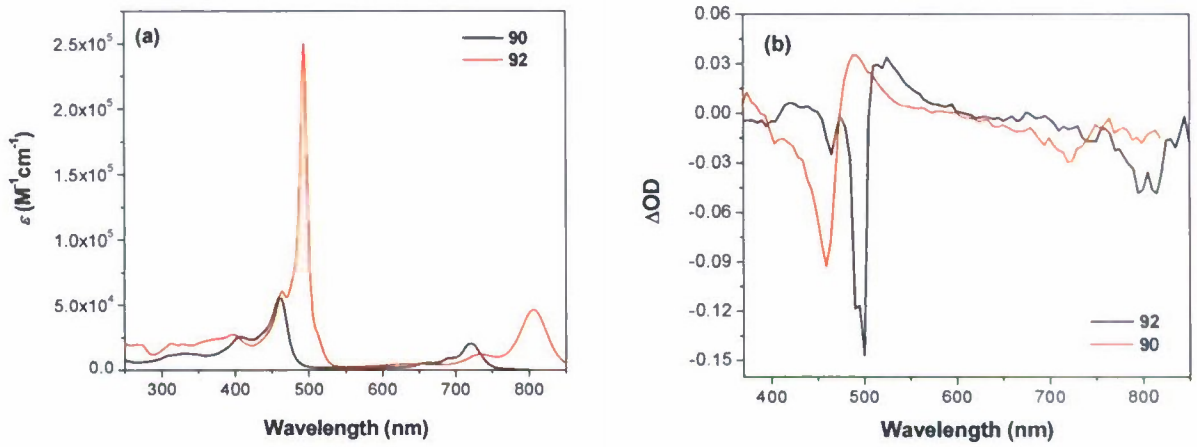

Figure 9. UV-vis (left) and triplet transient absorption (right) of **90** and **92** in methanol solutions. The excitation wavelength for the TA measurement was 355 nm.

Table 14. The photophysical parameters of the expanded porphyrin complexes **88**, **90** and **92** in methanol.

	λ_{abs} / nm	λ_f / nm (ϕ_f)	$\lambda_{T_1\text{-}T_n}$ / nm (ε_T /M^{-1}cm^{-1})	τ_T (μs)	ϕ_T
88	693	-	490 (2.28×10^4)	10.5	0.02
90	720	734 (0.019)	490 (5.36×10^4)	1.93	0.56
92	806	825 (0.029)	510 (2.9×10^4)	2.21	0.78

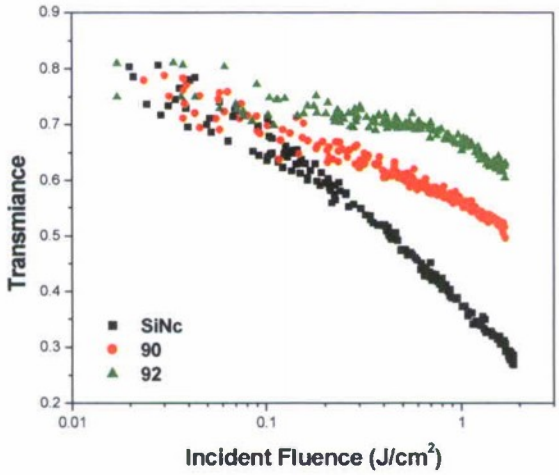

Figure 10. Nonlinear transmission of **90** in CH_3OH and **92** in $CHCl_3$ for 4.1 ns laser pulses in a 2-mm cuvette. The linear transmission was adjusted to 80%.

A.4. Synthesis and photophysical studies of stilbazolium derivatives

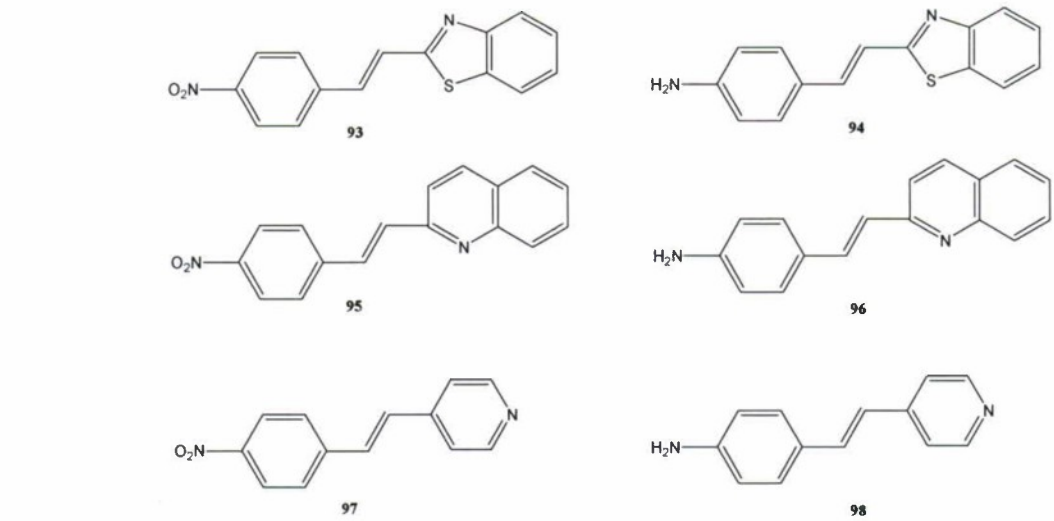

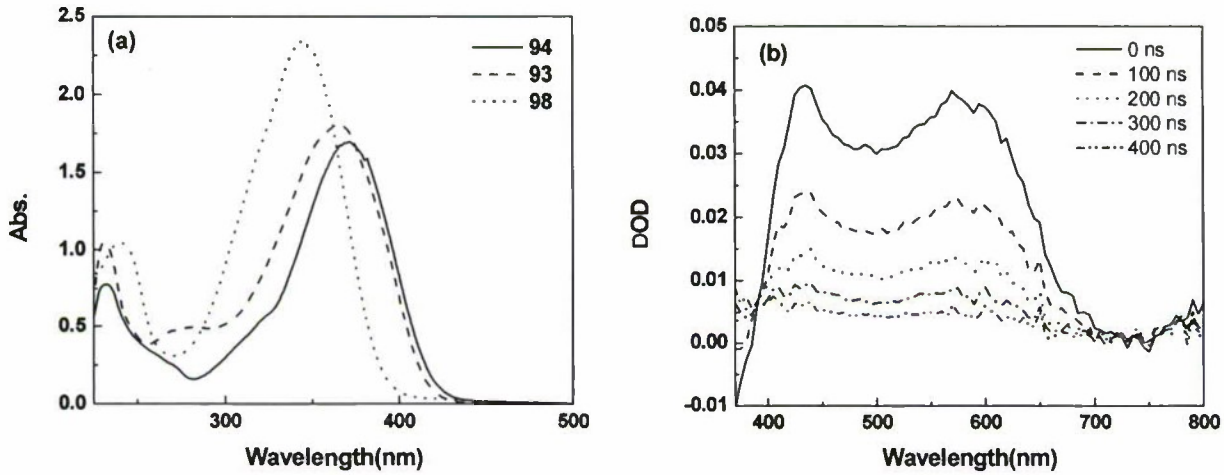

Figure 11. (a) UV-vis spectra of **93**, **94** and **98** in CH_2Cl_2 in a 1-cm cell. (b) Time-resolved transient difference absorption spectra of **93** in CH_2Cl_2. λ_{ex} = 355 nm.

The PI's previous work demonstrated that some of the stilbazolium derivatives exhibit moderate two-photon absorption in the near-IR region (W. Sun, F. Guo, D. Martyshkin, S. Mirov, C.-L. Zhan, D. Wang, *Proc. SPIE* Vol. **5211**, 75 (2003)). To evaluate how the strength of electron acceptor influences the nonlinear absorption and whether it is possible to combine the TPA/ESA from stilbazolium derivatives and the ESA from the Pt(II) complexes to obtain materials with broadband nonlinear transmission, we synthesized six stilbazolium derivatives (**93** – **98**) and studied their photophysics and nonlinear absorption. The UV-vis spectra of these compounds red-shift with increased conjugation and increased electron-withdrawing ability of the acceptor (Figure 11). However, the band maxima are all below 400 nm. No measurable ground-state absorption was observed for these compounds at 532 nm. Therefore, although compound **93** exhibit a broad positive transient absorption band in the visible region with a triplet lifetime of

~180 ns, no obvious nonlinear transmission was observed for ns laser pulses at 532 nm due to no sufficient triplet excited state population. Nevertheless, in view of the broad transient absorption band of **93** in the visible region and the linear absorption tail from 400 nm to 450 nm, **93** could possibly be useful for nonlinear transmission in the blue spectral region, which needs to be tested in the future. Moreover, the two-photon absorption characteristics of these compounds need to be investigated in the near future.

A.5. Photophysical and nonlinear absorption studies of zinc phthalocyanine derivatives

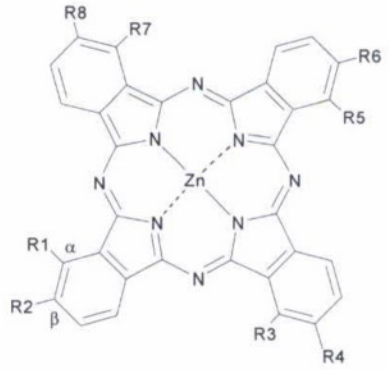

99 R_1 = O–(C6H4)–COOH; $R_2 = R_3 = R_4 = R_5 = R_6 = R_7 = R_8 = H$;

100 R_1 = O–(C6H4)–COOH (COOH at ortho); $R_2 = R_3 = R_4 = R_5 = R_6 = R_7 = R_8 = H$;

101 R_1 = O–(C6H4)–COOH (COOH at meta); $R_2 = R_3 = R_4 = R_5 = R_6 = R_7 = R_8 = H$;

102 R_2 = O–(C6H4)–COOH (COOH at meta); $R_1 = R_3 = R_4 = R_5 = R_6 = R_7 = R_8 = H$;

103 R_2 = O–(C6H4)–COOH (COOH at ortho); $R_1 = R_3 = R_4 = R_5 = R_6 = R_7 = R_8 = H$;

104 $R_2 = R_4 = R_6 = R_8$ = O–(C6H4)–COOH; $R_1 = R_3 = R_5 = R_7 = H$

105 $R_1 = R_3 = R_5 = R_7$ = O–(C6H4)–COOH; $R_2 = R_4 = R_6 = R_8 = H$

106 $R_1 = R_3 = R_5 = R_7$ = O–(C6H4)–COOH (COOH at meta); $R_2 = R_4 = R_6 = R_8 = H$

107 $R_1 = R_3 = R_5 = R_7$ = O–(C6H4)–$C_5H_{11}OOC$; $R_2 = R_4 = R_6 = R_8 = H$

108 $R_1 = R_3 = R_5 = R_7$ = O–(C6H4)–HOOC; $R_2 = R_4 = R_6 = R_8 = H$

Metallophthalocyanines have long been recognized as promising nonlinear transmission materials. However, many of the work were focused on the phthalocyanines with heavy metal center. The nonlinear absorption of ZnPc was not well studied, especially how the number of peripheral substituent(s) and the location of substituent(s) have not been well understood. In collaboration with Prof. Jiandong Huang at Fuzhou University, China, we systematically investigated the photophysics and nonlinear absorption of a series of ZnPc derivatives with different types, numbers and locations of peripheral substituent(s). The photophysical studies reveal that the peripheral substituted ZnPc derivatives exhibit low ground-state absorption, but strong triplet excited-state absorption from 400 to 580 nm with a longer triplet excited state lifetime in comparison to the unsubstituted ZnPc. These complexes all exhibit reverse saturable absorption for ns and ps laser pulses at 532 nm, and show broadband nonlinear absorption from 470 nm to 550 nm for ps laser pulses. Additionally, they all suppress the transmission of 532-nm

ns laser pulses better than ZnPc. Most importantly, our studies demonstrate that both the number and the position of the peripheral substituents dramatically affect the photophysics and nonlinear absorption of this type of materials. α-tetrasubstitution causes bathochromic shifts in the ground-state absorption spectra, the fluorescence spectra, and the triplet transient difference absorption spectra, and it also enhances the triplet excited-state absorption coefficients and increases the ratios of the triplet excited-state absorption to the ground-state absorption cross sections. All these features suggest that the peripheral substituted ZnPc derivatives are very promising nonlinear transmission materials. The detailed study of complexes **99 – 108** was reported in publication #19. The key photophysical and nonlinear absorption data as well as the spectra for these complexes are provided in Tables 15 – 17 and shown in Figures 12 – 14.

Table 15. Photophysical data of ZnPc derivatives in DMSO.

	λ_{abs} /nm (ε/ 10^4 l.mol^{-1}.cm^{-1}, f [a])	λ_f /nm (τ_s /ns, Φ_f)	λ_{T1-Tn}/nm (ε_{T1-Tn} / 10^4 l.mol^{-1}.cm^{-1})	τ_T /μs	τ_{isc} /ns[b]	Φ_T	Φ_Δ[c]
ZnPc	343 (5.88, 1.59), 672 (24.0, 0.44)[d]	684 (3.66, 0.23[e])	480 (3.00±0.10)[e]	123±9	5.63	0.65±0.02[e]	0.67[f]
99	346 (7.21, 1.99), 677 (26.3, 0.51)	684 (3.01, 0.14)	500 (5.02±0.05)	200±9	7.92	0.38±0.01	0.18
100	345 (5.31, 1.58), 677 (19.0, 0.37)	684 (3.11, 0.12)	480 (3.70±0.28)	168±27	6.35	0.49±0.04	0.17
101	346 (5.80, 1.99), 678 (21.3, 0.41)	684 (3.10, 0.11)	480 (4.31±0.31)	170±18	7.75	0.40±0.03	0.19
102	349 (8.45, 2.40), 675 (28.2, 0.61)	680 (3.17, 0.15)	480 (4.82±0.49)	181±27	7.93	0.40±0.04	0.14
103	349 (6.37, 1.59), 674 (21.1, 0.46)	680 (3.27, 0.16)	480 (3.82±0.15)	161±40	7.98	0.41±0.02	0.15
104	356 (7.13, 1.57), 678 (18.5, 0.44)	686 (3.00, 0.10)	500 (2.96±0.11)	238±40	6.12	0.49±0.02	0.17
105	340 (3.75, 1.20), 371 (3.63, 0.29), 692 (20.9, 0.44)	700 (2.70, 0.06)	560 (11.1±0.48)	215±21	7.11	0.38±0.02	0.31
106	341 (4.29, 1.91), 371 (4.20, 0.17), 693 (20.2, 0.47)	700 (2.70, 0.06)	560 (12.1±0.35)	174±21	6.59	0.41±0.01	0.30
107	337 (3.79, 1.17), 372 (3.83, 0.33), 696 (20.4, 0.44)	702 (2.59, 0.06)	560 (20.4±0.82)	142±8	10.4	0.25±0.01	0.36
108	340 (4.33, 1.62), 374 (4.29, 0.35), 697 (21.7, 0.50)	704 (2.83, 0.06)	560 (18.4±1.17)	140±5	11.8	0.24±0.02	0.39

[a] Oscillator strength, $f = 4.3\times10^{-9} \times \int \nu d\nu$. [b] $\tau_{isc} = \tau_s/\Phi_T$. [c] The uncertainty is ±0.01. [d] From Ref. 28. [e] From Ref. 22. [f] From Ref. 31

Table 16. Excited-state absorption cross-sections of ZnPc derivatives in DMSO measured by open-aperture Z-scans at 532 nm.

Complex	$\sigma_g/10^{-18}$ cm^2	$\sigma_s/10^{-17}$ cm^2	$\sigma_T/10^{-17}$ cm^2	σ_s/σ_g	σ_T/σ_g
99	3.1	4.0±0.5	18.0±2.0	13	58
100	2.4	4.0±0.5	10.5±2.0	17	44
101	2.5	4.5±0.5	7.0±1.5	18	28
102	3.7	4.5±0.8	11.0±2.0	12	30
103	3.1	4.5±0.5	6.0±1.5	15	19
104	4.0	4.0±0.6	4.5±1.0	10	11
105	1.6	3.0±0.5	17.0±2.0	19	106
106	2.3	1.8±0.4	18.0±2.5	8	78
107	1.3	1.8±0.2	40.0±4.0	14	308
108	1.8	3.0±0.5	28.0±3.0	17	156

Table 17. Wavelength-dispersion of the singlet excited-state absorption cross-section for complex **103** in DMSO measured by ps open-aperture Z-scans.

λ/nm	$\sigma_g/10^{-19}$ cm^2	$\sigma_s/10^{-17}$ cm^2	σ_s/σ_g
470	4.6	4.0±0.8	87
500	5.5	3.2±0.6	58
532	31.0	4.5±0.5	15
550	76.0	4.0±1.0	5

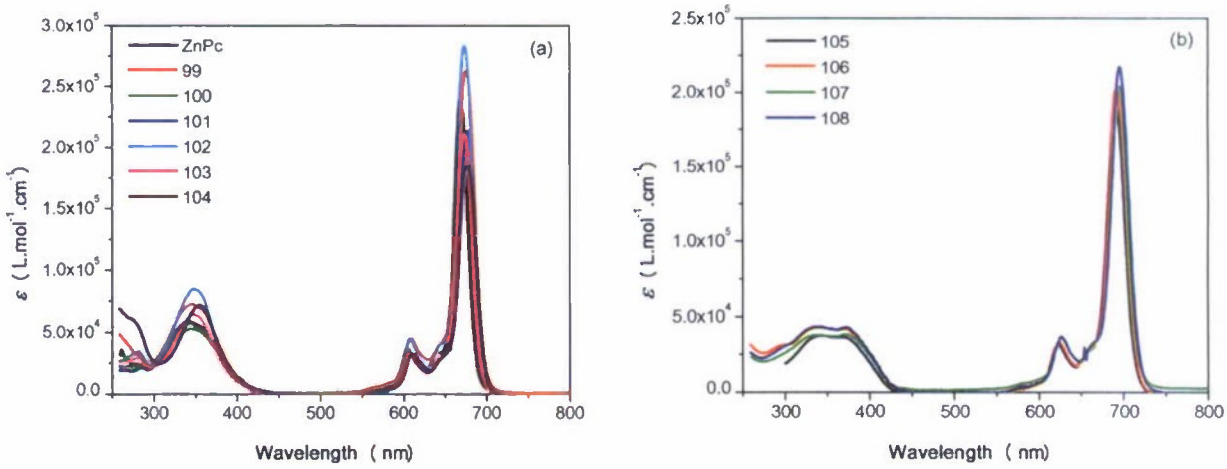

Figure 12. UV-vis absorption spectra of ZnPc derivatives in DMSO. (a) ZnPc and complexes **99-104**; (b) complexes **105-108**.

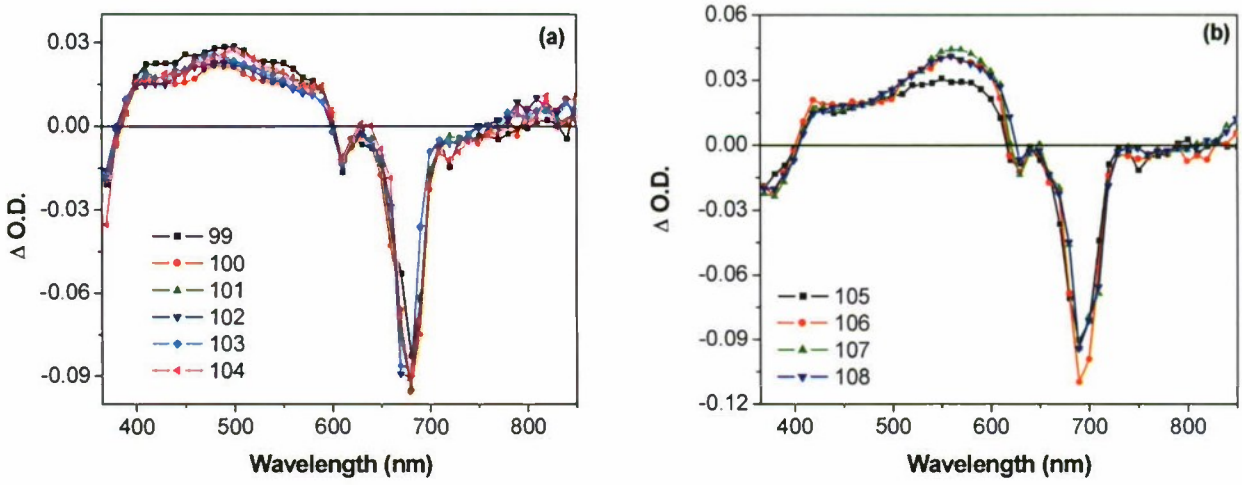

Figure 13. Triplet transient difference absorption spectra of the ZnPc derivatives immediately after the excitation. λ_{ex} = 355 nm, the excitation is provided by the 4.1 ns (FWHM) Nd:YAG laser. (a) Complexes **99-104**; (b) Complexes **105-108**.

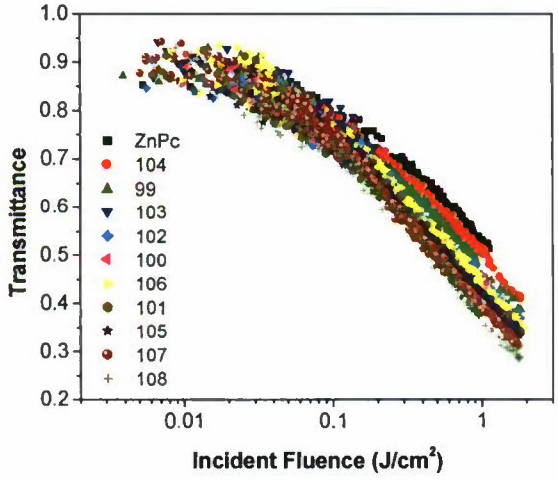

Figure 14. Nonlinear transmission curves for ZnPc derivatives and ZnPc at 532 nm for 4.1 ns (FWHM) laser pulses. The sequence of the legend labels goes from the worst nonlinear absorber (ZnPc) to the best one (complex **108**). The linear transmission for all samples was adjusted to 90±0.2% in a 2-mm cuvette.

B. Publications and Presentations

Based on the work described in section A, we have published 21 peer-reviewed journal papers and made 17 conference presentations. The list of our publications and presentations are provided below.

B.1. Peer-Reviewed Journal Publications

1. P. Shao, Y. Li, J. Yi, T. M. Pritchett, W. Sun*, "Cyclometalated Platinum 6-Phenyl-4-(9,9-dihexylfluoren-2-yl)-2,2′-bipyridine Complexes: Synthesis, Photophysics and Nonlinear Absorption", *Inorg. Chem.* **49**, 4507-4517 (2010).
2. J. Yi, B. Zhang, P. Shao, Y. Li, W. Sun*, "Synthesis and Photophysics of Platinum(II) 6-Phenyl-4-(9,9-dihexylfluoren-2-yl)-2,2′-bipyridine Complexes with Phenothiazinyl Acetylide Ligand", *J. Phys. Chem. A* **114**, 7055-7062 (2010).
3. T. M. Pritchett*, W. Sun, B. Zhang, M. J. Ferry, Y. Li, J. E. Haley, D. Mackie, W. Shensky, A. G. Mott, "Excited-state absorption of a bipyridyl platinum(II) complex with alkynyl-benzothiazolylfluorene units", *Opt. Lett.* **35**(9), 1305-1307 (2010).
4. W. Sun*, Y. Li, T. M. Pritchett, Z. Ji, J. Haley, "Excited-state absorption of 4′-(5‴-R-pyrimidyl)-2,2′:6′,2″-terpyridyl platinum(II) phenylacetylide complexes", *Nonlinear Optics, Quantum Optics: Concepts in Modern Optics* **40**, 163-174 (2010).
5. Z. Ji, Y. Li, T. M. Pritchett, N. S. Makarov, J. E. Haley, Z. Li, M. Drobizhev, A. Rebane, W. Sun*, "Photophysics and Two-photon Absorption of 4-[9,9-Di(2-ethylhexyl)-7-diphenylaminofluoren-2-yl]-2,2′:6′,2″-terpyridine and Their Platinum Chloride Complexes", accepted by *Chem. Eur. J.* (2010).
6. W. Sun*, B. Zhang, Y. Li, T. M. Pritchett, Z. Li, J. E. Haley, "Broadband Nonlinear Absorbing Platinum 2,2′-Bipyridine Complex Bearing 7-(Benzothiazol-2′-yl)-9,9-diethyl-2-ethynylfluorene Ligands", *Chem. Mater.* ASAP released on web on 11/9/2010.
7. R. Liu, Y. Li, Y. Li, H. Zhu, W. Sun,* "Photophysics and Nonlinear Absorption of Cyclometalated Platinum(II) 6-Phenyl-2,2'-bipyridyl Complexes with Different Acetylide Ligands", *J. Phys. Chem. A* ASAP released on web on 11/15/2010.
8. Y. Li, T. M. Pritchett, J. Huang, M. Ke, W. Sun*, "Nonlinear refraction of peripheral-substituted zinc phthalocyanines investigated by nanosecond and picosecond Z-scan", submitted to *Opt. Mater.* (2010).
9. P. Shao, Y. Li, A. Azenkeng, M. Hoffmann, W. Sun*, "Influence of Alkoxyl Substituent on 4,6-Diphenyl-2,2'-bipyridine Ligand on Photophysics of Cyclometalated Platinum(II) Complexes: Admixing Intraligand Charge Transfer in Low-lying Excited States", *Inorg. Chem.* **48**(6), 2407-2419 (2009).
10. I. Mathew, W. Sun*, "Photophysics of Pt(II) 4,6-Dipheny-2,2'-bipyridyl Complexes in Solution and LB Film", *J. Organometallic Chem.* **694**, 2750-2756 (2009).
11. H. Zhang, B. Zhang,Y. Li, W. Sun,* "Acid-Sensitive Pt(II) 2,6-Di(pyridin-2-yl)pyrimidin-4(1*H*)-one Complexes", *Inorg. Chem.* **48**(8), 3617-3627 (2009).

12. Z. Ji, A. Azenkeng, M. Hoffmann, W. Sun*, "Synthesis and Photophysics of 4'-R-2,2';6',2''-terpyridyl (R = Cl, CN, $N(CH_3)_2$) Platinum(II) Phenylacetylide Complexes", *Dalton Trans.* 7725-7733 (2009).
13. Y. Li, T. M. Pritchett, P. Shao, J. Haley, H. Zhu, W. Sun*, "Excited-state absorption of *mono-*, *di-* and *tri*-nuclear cyclometalated platinum 4,6-diphenyl-2,2'-bipyridyl complexes", *J. Organometallic Chem.* **694**, 3688-3691 (2009).
14. T. Lu, P. Shao, I. Mathew, A. Sand, W. Sun*, "Synthesis and Photophysics of Benzotexaphyrin: A Near-IR Photosensitizer and Emitter", *J. Am. Chem. Soc.* **130**(47), 15782-15783 (2008).
15. Y. Li, D. Dini, M. J. F. Calvete, M. Hanack, W. Sun*, "Photophysics and Nonlinear Optical Properties of Tetra- and Octabrominated Silicon Naphthalocyanines.", *J. Phys. Chem. A.* **112**(3), 472-480 (2008).
16. P. Shao, Y. Li, W. Sun*, "Cyclometalated platinum(II) complex with strong and broadband nonlinear optical response", *J. Phys. Chem. A.* **112**(6), 1172-1179 (2008).
17. P. Shao, Y. Li, W. Sun*, "Platinum(II) 2,6-bis(2'-pyridyl)-4-(4'-tolyl)-1,3,5-triazyl complexes: synthesis and photophysics", *Organometallics* **27**(12), 2743-2749 (2008).
18. T. M. Pritchett*, W. Sun, F. Guo, B. Zhang, M. J. Ferry, J. E. Rogers-Haley, W. Shensky III, A. G. Mott, "Excited state absorption and photophysical parameters of a terpyridyl platinum(II) pentynyl complex", *Opt. Lett.* **33** (10), 1053-1055 (2008).
19. Y. Li, T. M. Pritchett, J. Huang, M. Ke, P. Shao, W. Sun*, "Photophysics and nonlinear absorption of peripheral substituted zinc phthalocyanines", *J. Phys. Chem. A* **112** (31), 7200-7207 (2008).
20. Z. Ji, Y. Li, W. Sun*, "4'-(5'''-R-Pyrimidyl)-2,2':6',2''-terpyridyl (R = H, Cl, Ph, CN, OEt) Platinum(II) Phenylacetylide Complexes: Synthesis and Photophysics", *Inorg. Chem.* **47**(17), 7599-7607 (2008).
21. P. Shao, W. Sun*, "Trinuclear platinum(II) 4,6-diphenyl-2,2'-bipyridine complex with bis(diphenylphosphinomethyl)phenylphosphine auxiliary ligand: synthesis, structural characterization and photophysics", *Inorg. Chem.* **46**(21) 8603-8612 (2007).

B.2. Conference Presentations

1. W. Sun, B. Zhang, Y. Li, T. M. Pritchett, J. E. Haley, "4-(7-Benzothiazolyl-9,9-diethylfluoren-2-yl) Substituted Terpyridyl Platinum Chloride Complexes with Broadband Nonlinear Absorption", presented at the *NSF Inorganic Workshop*, May 18-21, Santa Fe, NM (2010).
2. W. Sun, B. Zhang, Y. Li, T. M. Pritchett, "Photophysics and broadband nonlinear absorption of platinum terdentate or diimine complexes", will be presented at *Pacifichem 2010*, Dec. 15-20, Honolulu, Hawaii (2010).
3. W. Sun, Z, Ji, Y. Li, T. M. Pritchett, N. S. Makarov, J. E. Haley, A. Rebane, "Two-photon Absorbing 4-(9,9-Di(2-ethylhexyl)-7-diphenylaminofluoren-2-yl)-2,2':6',2"-terpyridine Platinum Complexes", will be presented at *Pacifichem 2010*, Dec. 15-20, Honolulu, Hawaii (2010).

4. W. Sun, "Nonlinear absorption of platinum(II) terdentate complexes", presented at the *International Symposium on Materials and Devices for Nonlinear Optics (ISOPL '5)*, Ile de Porquerolles, June 26 – July 1, 2009 (Invited)
5. Z. Ji, A. Azenkeng, M. R. Hoffmann, W. Sun,* "Synthesis and photophysics of 4'-R-2,2';6',2''-terpyridyl (R=Cl, CN, $N(CH_3)_2$) Platinum(II) Phenylacetylide Complexes", presented at *the Inter-America Photochemical Society Winter Conference*, St. Petersburg, FL, Jan. 2-5, 2009.
6. W. Sun, P. Shao, Y. Li, "Photophysics and nonlinear absorption of platinum biphenyldipyridyl complexes with an alkoxyl substituent", presented at the *SPIE Annual Conference: Optics and Photonics,* San Diego, CA, August 13, 2008.
7. W. Sun, T. Lu, P. Shao, I. Mathew, A. Sand, "Cadmium Benzotexaphyrin and lanthanide texaphyrins: Synthesis and photophysics", presented at the *4th Sino-US Symposium on Organic Chemistry*, Beijing, China, June 12-13, 2008. (Invited)
8. W. Sun, "Platinum terdentate complexes as broadband nonlinear transmission materials", presented at the *Tri-Service Information Exchange Conference*, Hilton Head Island, SC, April 13-16, 2008.
9. W. Sun, P. Shao, Y. Li, I. Mathew, "Photophysical and Nonlinear Optical Properties of Mononuclear and Dinuclear Platinum(II) Complexes with 4,6-Diphenyl-2,2'-bipyridine Ligand", presented at *the Inter-America Photochemical Society Winter Conference*, St. Petersburg, FL, Jan. 3-6, 2008.
10. P. Shao, W. Sun, "Synthesis of a New Series of Cyclometalated Platinum(II) Complexes for Nonlinear Transmission Application", presented at *the Inter-America Photochemical Society Winter Conference*, St. Petersburg, FL, Jan. 3-6, 2008.
11. Z. Ji, W. Sun, "Synthesis and Photophysics of 4'-(5'''-R-Pyrimidyl)-2,2';6',2''-terpyridine Platinum(II) Phenylacetylide Complexes (R=H, Cl, Ph, CN, OEt)", presented at *the Inter-America Photochemical Society Winter Conference*, St. Petersburg, FL, Jan. 3-6, 2008.
12. W. Sun, P. Shao, Y. Li, "A square-planar platinum complex with large and broadband nonlinear optical response", presented at *the First Asian Conference on Coordination Chemistry*, Okazaki, Japan, July 31, 2007. (Invited)
13. W. Sun, "Platinum terdentate complexes: Synthesis, photophysics and applications", presented at the *3rd Sino-US Organic Chemistry Symposium*, Wuhan, China, June 1-2, 2007. (Invited)
14. P. Shao, W. Sun, "Synthesis, photophysics, and optical limiting of a trinuclear cyclometalated Pt(II) complex", presented at the *233rd ACS Annual Meeting*, Chicago, IL, March 25-28, 2007.
15. P. Shao, W. Sun, "A new cyclometalated Pt(II) complex with strong nonlinear absorption", presented at the *233rd ACS Annual Meeting*, Chicago, IL, March 25-28, 2007.
16. W. Sun, P. Shao, "Photophysics and nonlinear transmission of a cyclometalated platinum(II) 4,6-diphenyl-2,2'-bipyridyl pentynyl complex", presented at the *MRS Annual Spring Meeting*, San Francisco, CA, April 9-13, 2007.
17. Timothy M. Pritchett, Michael J. Ferry, Andrew G. Mott, William Shensky III, Fengqi Guo, Bingguang Zhang, Wenfang Sun, "Excited state absorption cross-sections of a novel

terpyridyl platinum(II) complex", presented at the *NLO-2007*, Honolulu, Hawaii, August 4, 2007.

C. Financial Report

During the award period (7/1/06 – 6/30/10), we have spent total $281,783.22 on salaries and fringe benefits for the PI, the postdoctors and graduate students involved in this project, $72,848.66 were spent on materials, supplies, instrument user fees and other operating expense. $17,194.12 was used for travel expense to professional conferences to present results. The total indirect cost was $158,862.